CRREL

Structure of Ordinary Ice I$_h$
Part II: Defects in Ice
Volume 1: Point Defects

Victor F. Petrenko and Robert W. Whitworth

April 1994

DTIC
ELECTE
DEC 05 1994
S G D

DTIC QUALITY INSPECTED 5

THE UNIVERSITY
OF BIRMINGHAM

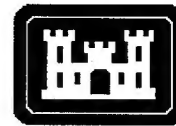THAYER SCHOOL OF ENGINEERING
1867

19941128 113

Abstract

This report examines point defects in ice: molecular defects (vacancies and interstitials), protonic point defects (ions and Bjerrum defects) and electronic point defects (solvated electrons and radicals). Experimental results and theoretical models of the defects' atomic and electronic structures, energies and mobilities are reviewed. Special attention is given to the results of studies from the last two decades. Among the experimental techniques under consideration are nuclear magnetic resonance, X-rays topography, electron spin resonance, measurements of ice conductivity and dielectric permittivity, spectra of optical absorption and photoluminescence, and measurements of diffusion coefficients of the oxygen and hydrogen isotopes in ice. Ab initio calculations, computer simulations, Jaccard's theory and soliton models are used to discuss the defects' structures and their properties.

Special Report 94-4

**U.S. Army Corps
of Engineers**
Cold Regions Research &
Engineering Laboratory

Structure of Ordinary Ice I$_h$
Part II: Defects in Ice
Volume 1: Point Defects

Victor F. Petrenko and Robert W. Whitworth

April 1994

PREFACE

FOREWORD

At the present time, thousands and thousands of people around the world deal with ice, snow and permafrost. They are scientists, educators, engineers, navigators, meteorologists and others. While a small fraction of these people contribute to the knowledge base in ice physics, all of them use knowledge from it frequently. Moreover, successful applied research is based upon fundamental science—one more reason for ice specialists to have a textbook on ice physics on their desks.

The first modern ice physics text was Fletcher's book on *The Chemical Physics of Ice* (1970). Fletcher's book is in typical textbook format: it is reasonably brief and easy to understand. He touched on a few of the most important topics, but not all of them.

The most comprehensive book on ice physics to date was published by Hobbs in 1974. Hobbs considered almost all of the basic aspects of ice as understood at that time. Moreover, he described and compared several (sometimes opposing) viewpoints. This fundamental and rather large (837 pages) book is commonly known as the "Ice Bible" by specialists in the field. In 1974 and 1975, two CRREL Monographs on ice were produced by John Glen. These were briefly and clearly written and reviewed almost all ice-related subjects. This work was (and in some respects still is) a magnificent introduction to ice.

Finally, in 1981 Maeno wrote a simple popular book for the express purpose of attracting people's attention to the subject.

During the past 20 years, a significant amount of new experimental and theoretical work has appeared, dramatically changing our views on ice physics. As a result, we are now able to formulate physical laws using more simple and direct methods. We have found some of the physical models used in the past to be completely wrong. The physics of ice is a much better developed subject than it was 20 years ago.

For the above reasons, we feel the time is ripe for a contemporary book on ice physics, incorporating the known and proven with almost 20 years worth of material not covered by previous works.

We have tried to prepare a "readable" book, and not one that requires the reader to be a uniquely educated person. It is our intent to present the material in such a way that any reader attracted by the title *Ice Physics* will be able to comprehend it. This is quite difficult for a book dedicated, not to a particular field of knowledge, but to a specific material. Indeed, for ice it means we have to consider a wide variety of subjects, including quantum chemistry, solid state physics, the theory of elasticity, ionic conductivity, synchrotron x-ray topography, crystal growth, the physics of surfaces and more.

The primary goal is to produce as simple a book as possible without sacrificing scientific accuracy. Experimental facts, physical ideas and theories will be strongly organized and bound together cohesively. The reader will be introduced to a wide variety of material on a step by step basis. Then the picture will be whole.

To accelerate materials publication, this book will appear first in the form of a series of joint CRREL–Dartmouth reports, later to be published in CRREL's Monograph series, on:

1. The structure of ordinary ice
   Part I: "Ideal" structure of ice. Ice crystal lattice
   Part II: Defects in Ice
   > Volume 1: Point defects
   > Volume 2: Dislocations and planar defects
2. Electrical properties of ice
   Part I: Conductivity and dielectric permittivity of ice
   Part II: Advanced topics and new physical phenomena
3. Optical properties
4. Electro–optical effects in ice

5. Thermal properties
6. Mechanical properties of ice. Elasticity and anelastic relaxation. Plastic properties. Fracture of ice
7. Electromechanical effects in ice
8. Surface of ice
9. Other forms of ice and their properties
10. Ice in space
11. Ice research laboratories

The reports will be prepared in a sequence convenient to the authors. The present report is the third in the series.

CONTENTS   Page

ILLUSTRATIONS

TABLES

NOMENCLATURE

a	lattice constant
$\mathbf{b}$	Burgers vector
D	diffusion coefficient
D_H	diffusion coefficient of hydrogen in ice
D_i	diffusion coefficient of interstitials
D_s	self-diffusion coefficient
D_{so}	$(va^2)\exp\left(\dfrac{S_v}{k_B}\right)$
D_v	diffusion coefficient of vacancies
$\vec{D}$	electric displacement vector
e	proton charge
ε	relative dielectric permittivity
ε	strain
E_{aB}	energy of creation of a pair of Bjerrum defects
E_{ai}	energy of creation of an ion pair
E_{as}	activation energy of static conductivity σ_s
$E_{a\infty}$	activation energy of high-frequency conductivity σ_∞
E_f	activation energy for defect creation
e_i	defects' electric charge ($i = 1, 2, 3, 4$)
E_{if}	formation energy of interstitials
E_G	forbidden gap width
E_k	kink formation energy
E_{mi}	activation energies of protonic defects' motion ($i = 1, 2, 3, 4$)
ε_o	dielectric permittivity of vacuum
E_s	activation energy of self-diffusion
ε_s	static dielectric permittivity ($\omega \ll \omega_D$)
$E_{\sigma i}$	activation energy of partial conductivity of i-type defects ($i = 1, 2, 3, 4$)
E_τ	activation energy of Debye relaxation time
$\vec{E}, E$	electric field strength
ε_∞	high-frequency ($\omega \gg \omega_D$) dielectric permittivity
$\dot{\varepsilon}$	strain rate
F	free energy
Φ	$= 3.85\, k_B T\, r_{oo}$
f, v	frequencies
F_d	free energy attributable to defect formation
F_k	free energy of kink formation
F_m	free energy of kink motion
F_i	force acting on i-type of defects
$\mathbf{g}$	diffraction vector
γ_{ai}	activation volume of formation of protonic defects
γ_{mi}	activation volume of protonic defects' motion
h	separation of the Peierls troughs
η_i	$= 1, -1, -1, 1$ for $i = 1, 2, 3, 4$
j_i	flux density of defects ($i = 1, 2, 3, 4$)
$\vec{J}_{dis}$	displacement current
$\vec{J}_{dr}$	drift current
J	electric current density
k_B	Boltzmann constant
$\mathbf{l}$	unit vector parallel to a dislocation line
μ	mobility
μ_i	mobility of i-type of defects
n	concentration (in m^{-3})
N	number of molecules
N_d	concentration of dislocations
n_D	D-defect concentration
n_{H2O}	concentration of water molecules in ice
n_i	concentration of defects ($i = 1, 2, 3, 4$)
n_k	number of kinks per unit length
n_L	L-defect concentration
n_v	concentration of vacancies
P	pressure
q, e_i	electric charge of carriers
$\dot{Q}$	rate of heat generation
r	distance
r_{oo}	oxygen–oxygen distance in ice lattice (2.76 (Å)
S	entropy
σ	conductivity
σ	normal stress
σ_B	Bjerrum defect conductivity—

$\sigma_B = \sigma_3 + \sigma_4$

S_c configurational entropy

S_f vibrational entropy

σ_i partial conductivity of "i" charge carrier

σ_{ion} ionic conductivity—$\sigma_{ion} = \sigma_1 + \sigma_2$

S_k kink entropy

σ_s static or low-frequency conductivity ($\omega \ll \omega_D$)

σ_∞ high-frequency conductivity ($\omega \gg \omega_D$)

T temperature

τ shear stress

t time

τ_b mean time to reorient a hydrogen bond

τ_D $= \omega_D^{-1}$ Debye relaxation time

τ_L lifetime of charge carriers

U internal energy

U_{im} activation energy of motion of interstitials

U_m activation energy of ionic motion

v_d dislocation velocity

$\vec{v}_d$ drift velocity

V_{if} activation volume of formation of interstitials

V_{im} activation volume of motion of interstitials

v_k kink velocity

V_{mol} molecular volume in ice—3.3×10^{-23} cm^3

W number of configurations of a system

ω circular frequency

ω_D Debye frequency

$\vec{\Omega}$ configurational vector

x $= n_i / n_{H_2O}$

y $= n_D / n_{H_2O}$

Structure of Ordinary Ice I$_h$
Part II: Defects in Ice
Volume 1: Point Defects

VICTOR F. PETRENKO AND ROBERT W. WHITWORTH

INTRODUCTION

Unlike most previous authors of books on ice physics (Hobbs 1974, Fletcher 1970, Glen 1974), we decided to isolate all kinds of defects in ice into separate reports. Such a division reflects, first, the important role that defects play in materials physics. While most of the physical properties of solids are structurally sensitive ones, in ice some of them are entirely determined by specific defects. For example, ion and Bjerrum defect fluxes are responsible for electrical properties and inelastic relaxation in ice (see, e.g., Petrenko and Ryzhkin 1984c). Second, it is in the study of defects (dislocations, point defects, grain boundaries) that significant progress has been achieved since the last monograph on ice physics was published (Hobbs 1974). Because of this, special attention will be given to the results of studies from the last two decades.

Following a tradition in materials science, we divide consideration of defects into three parts: point defects, dislocations and planar defects. In this report we discuss the structure and physical properties of zero-dimensional defects, known as point defects. In the second report, entitled *Structure of Ordinary Ice I$_h$; Part II: Defects in Ice; Volume 2: Linear and Planar Defects*, we consider dislocations that are one-dimensional defects, and, finally, grain boundaries and stacking faults (two-dimensional defects) will be described. The structure and properties of another two-dimensional "defect"—the surface—are treated in a separate report.

GENERAL CONSIDERATION OF POINT DEFECTS

We begin our review of defects in ice with the smallest and simplest ones. These are the point defects that are usually vacancies, interstitials, impurity atoms, bivacancies, Schottky and Frenkel pairs, etc., but in ice also include special kinds of defects associated with the disorder of the hydrogen atoms. The term "point" does not, of course, mean that the defects do not have a size, but that they are located at a specific point within the crystal. They are usually located within one or two unit cells, although elastic deformation produced by the defects can spread to much larger distances.

Point defects in ice (as in other solids) play a fundamental role in many physical processes such as diffusion, anelastic relaxation, electrical conductivity, dielectric permittivity and optical absorption. They differ from one another in structure, concentration and mobility, but in this introduction we will consider some general results applicable to them all. These are the relationships between concentration, formation energy, jump rates, diffusion coefficient and mobility.

Since, for a given number of molecules the arrangement with minimum energy is perfect, with no defects, some additional energy E_f is required to produce a defect. For the majority of point defects in ice, E_f is of the order of 0.5 eV. These values are much greater than the average energy of thermal vibration, $k_B T \approx 0.023$ eV (–10°C), so that at first sight the formation of these defects is unjustified. However, according to thermodynamics at constant temperature and constant volume, thermal equilibrium is attained at minimum free energy F rather than at minimum internal energy U, where

$$F = U - TS. \tag{1}$$

The appearance of defects increases the internal energy U, but, because of the large number of different ways in which the defects can be located in the crystal, their entropy increases more rapidly, and the minimum of F occurs at a finite defect concentration.

We can illustrate this point with a simple example. Consider a crystal lattice consisting of N identical points (atoms, molecules or elementary cells). A point defect with energy of formation E_f

could appear with equal probability at any of the points. Then, the free energy attributable to the formation of n defects will be

$$F_d = E_f n - TS_c \qquad (2)$$

where S_c is the configurational entropy of the n defects in the lattice

$$S_c = k_B \ln W \qquad (3)$$

and W is the number of arrangements of n identical defects over these N identical sites

$$W = \frac{N!}{n!(N-n)!} . \qquad (4)$$

At equilibrium

$$\frac{\partial F_d}{\partial n} = 0 \qquad (5)$$

and substituting eq 2–4 into eq 5 and using the Stirling formula—$\ln(N!) \approx N \ln N - N$ for $N \gg 1$—we obtain

$$\frac{n}{N-n} = \exp\left(-\frac{E_f}{k_B T}\right). \qquad (6)$$

Assuming $E_f \gg k_B T$, we obtain

$$n \approx N \exp\left(-\frac{E_f}{k_B T}\right). \qquad (7)$$

To be more precise, the appearance of a point defect not only changes the configurational entropy, it also affects the vibrational entropy because of a slight change in the elastic lattice vibration spectrum. This vibrational entropy change S_f would lead to an additional factor of $\exp(S_f/k_B)$ in eq 7 so that

$$n \approx N \exp\left(\frac{S_f}{k_B}\right) \exp\left(-\frac{E_f}{k_B T}\right). \qquad (8)$$

Calculations of S_f for defects are quite difficult, and are far beyond this approach. We indicate here only that, according to experimental results, the ratio S_f/k_B may not be small and must be taken into account.

The majority of point defects in ice have a high mobility at "not too low" ($T \geq 100$ K) temperatures, migrating from one lattice site to another by jumping. The equilibrium positions of point defects in the lattice are separated by potential energy barriers of height U_m, and motion occurs by thermally

activated hops over these barriers. Let us consider the motion of some electrically charged defect with charge q, which we will refer to, for brevity, as an "ion."

The simple case of the one-dimensional motion of such an ion is shown in Figure 1. To move one interatomic distance in the direction of the field E, the positive ion would need an activation energy $U_m - qEa/2$, and to move against the field, it would need $U_m + qEa/2$. The frequency of ion jumps in the direction of the field is expressed by

$$f_1 = \nu \exp\left\{-\frac{U_m - qaE/2}{k_B T}\right\} \qquad (9)$$

and against the field by

$$f_2 = \nu \exp\left\{-\frac{U_m - qaE/2}{k_B T}\right\} \qquad (10)$$

where ν is related to the frequency of oscillations of the ion in its potential well. Since every jump moves the ion over the distance a, the mean drift velocity of the ion in the direction of the field becomes

$$\langle v_d \rangle = a\,(f_1 - f_2) = 2\nu\,a\,\exp\left(-\frac{U_m}{k_B T}\right) \sinh\left(\frac{qEa}{2k_B T}\right). \qquad (11)$$

Since usually

$$q\,E\,a \ll 2\,k_B T \qquad (12)$$

we can substitute sinh with its argument in eq 11

$$\langle v_d \rangle = \left[\left(\frac{\nu q a^2}{k_B T}\right) \exp\left(-\frac{U_m}{k_B T}\right)\right] E. \qquad (13)$$

Thus, the ion mobility, which is defined as the ratio between drift velocity and electric field strength E, will be

$$\mu = \left(\frac{\nu q a^2}{k_B T}\right) \exp\left(-\frac{U_m}{k_B T}\right) \qquad (14)$$

and is independent of E. U_m is called the activation energy of migration.

The quantity

$$\nu_h = \frac{1}{2} \nu \exp\left(-\frac{U_m}{k_B T}\right). \qquad (15)$$
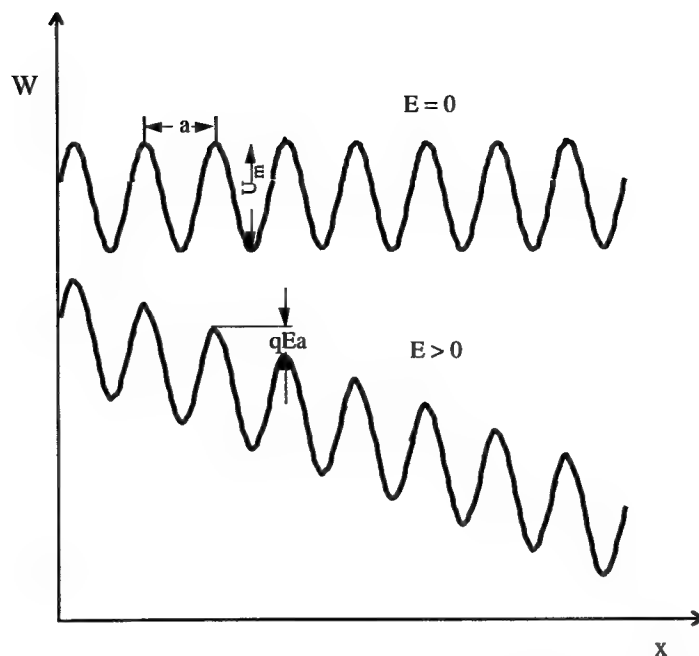
Figure 1. Potential energy of an ion in a crystal lattice W as a function of coordinate x with (E > 0) and without (E = 0) an electric field; a is an interatomic distance.

represents the probability of jumping or the mean number of jumps in a given direction per second, and the diffusion coefficient of the ions is $D = \nu_h a^2$. For chaotic thermal motion of this kind, the mobility μ and the diffusion coefficient D are always related by the Einstein relation

$$\frac{\mu}{D} = \frac{|q|}{k_B T} \tag{16}$$

so that

$$D = (\nu a^2) \exp\left(-\frac{U_m}{k_B T}\right). \tag{17}$$

Equation 17, which does not contain q, is of course also valid for neutral defects such as vacancies and interstitials and for neutral atoms and molecules dissolved in ice. When the above simple formulae are for some reason not able to describe the motion or concentration of some specific defect in ice, we shall perform an additional analysis.

MOLECULAR DEFECTS

The principal molecular point defects in ice are vacancies and interstitials. A *vacancy* is a site from which a water molecule is missing, and an *interstitial* is an extra molecule inserted in a space be-

tween the normal molecules of the structure. These defects can clearly be formed in pairs by the displacement of a molecule off its normal lattice site to an interstitial position, but they can also be formed independently. For example, a vacancy appears when we remove a water molecule from its regular position and place it on the surface. Dislocations and grain boundaries can also emit or absorb vacancies and interstitials.

In thermal equilibrium at a given temperature, the defect concentrations are determined by their formation energy E_f (and any associated entropy S_f). To a first approximation, the energy required to form a vacancy is equal to the energy required to remove a molecule from the bulk of the crystal and place it at a kink on a surface step. In so doing, the number of hydrogen bonds per molecule is reduced from four to two.* Subsequently, there will be an elastic relaxation of the lattice around the vacant site, which slightly lowers the energy.

The formation of an interstitial, on the other hand, involves the transfer of a molecule from a

---

*Devlin (1992a) recently found from spectroscopic data that the surface molecules of crystalline ice are three-coordinate bonded, i.e., there is only one, not two, dangling O-H bond per molecule. Nevertheless, if a crystal is built up by adding molecules to the surface, the number of bonds is two, irrespective of the number of dangling bonds at the surface.

kink site on the surface to an interstitial position. This again breaks two hydrogen bonds and involves a short-range repulsive interaction among nearest neighbors and an elastic distortion of the surrounding lattice. These considerations suggest that the energy of formation of these defects will be of about the same magnitude as the cohesive energy per molecule, which is known to be 0.6 eV.

More accurate calculations using computer simulations were made by Cotteril et al. (1973). In their work they used a realistic potential of interaction between water molecules introduced by Ben-Naim and Stillinger (1972). Their calculations were only restricted by their assumption that the molecules were absolutely rigid and the small size of the molecular cluster used in their model. The energies of molecular point defects (and also of the Bjerrum L- and D-defects to be described later) calculated by Cotteril et al. are summarized in Table 1.

Water molecules can diffuse through ice by either a vacancy or an interstitial process. To be specific, let us consider such self-diffusion as occurring by the motion of vacancies. The diffusion flux of vacancies j_v is given by the formula

$$j_v = -D_v \, \text{grad}(n_v) \tag{18}$$

where D_v is the diffusion coefficient of vacancies defined in eq 17 and n_v is the vacancy concentration. A particular water molecule in the ice can migrate by vacancy diffusion only if one of its nearest-neighbor lattice sites happens to be vacant. Consequently, the coefficient of self-diffusion of molecules D_s is much smaller than the coefficient of vacancy diffusion

Table 1. Defect formation energy (eV) in ice (after Cotteril et al. 1973).

| Defect | Cluster size and elastic relaxation | | |
	16, unrelaxed	16, relaxed	432, unrelaxed
Cohesive energy	0.466	—	0.465
Vacancy	0.466	0.447	0.465
L-defect	0.467	0.388	0.403
D-defect	0.491	0.407	0.428
Interstitial	0.616	0.528	0.695

$$D_s = \frac{n_v}{n_{H_2O}} D_v . \tag{19}$$

In practice, the self-diffusion coefficient of a material can be determined using a tracer technique, provided that the material possesses suitable, usually radioactive, isotopes. For ice, three isotopes have been used in such diffusion measurements: deuterium, ^2H; tritium, ^3H; and ^{18}O. The general procedure is to place a known concentration of the isotope onto one end of a block of ice, which is then left at a fixed temperature for a certain period of time. The distribution of the isotope along a particular axis is then measured experimentally. Table 2 and Figure 2 summarize the results from such experiments.

If we substitute eq 8 and 17 into eq 19, we obtain

$$D_s = D_{s0} \exp\left(-\frac{E_s}{k_B T}\right) \tag{20}$$

in which

$$D_{s0} = (va^2) \exp\left(\frac{S_v}{k_B}\right) \tag{21}$$

and

$$E_s = E_f + U_m . \tag{22}$$

Several trends in the experimental data in Table 2 are of interest. First, the diffusion coefficients of oxygen and hydrogen isotopes, as well as their activation energies, are approximately equal. This is major evidence that in ice oxygen and hydrogen diffuse cooperatively by the diffusion of whole water molecules. The scatter in D_s and E_s (relatively small) could be caused by different degrees of imperfection of the ice used. For the majority of solids, it has been established that the diffusion rate along grain boundaries or along dislocation lines considerably exceeds the bulk rate. Hence, one could expect larger values of D_s in polycrystalline ice and in ice with high dislocation density (which was unknown in the papers cited).

The key question in the study of self-diffusion in ice is about whether the process occurs by the motion of vacancies or interstitials. Since, in the majority of crystals vacancies dominate interstitials, self-diffusion in ice was for a long time also explained in terms of vacancy diffusion. However, experiments by Higashi, Hondoh and others during last decade have clearly proven that the dominant process in diffusion in ice is that ascribable to interstitials. Their experiments involved the careful study of the growth and annealing of dislocation loops produced by rapid cooling.

4

Table 2. Self-diffusion coefficient D_s and its activation energy E_s in ice.

Measurement	Self diffusion coefficient D_s ($m^2 s^{-1}$) at $-10°C$	Activation energy E_s (eV)	Reference
Oxygen-18 in polycrystalline ice.	1.0×10^{-14} (at $-1.8°C$)	—	Kuhn and Thürkauf (1958)
Deuterium in polycrystalline ice.	1.0×10^{-14} (at $-1.8°C$)	—	Kuhn and Thürkauf (1958)
Tritium perpendicular to c-axis in artificial single crystals.	1.53×10^{-15}	0.58 ± 0.05	Dengel and Riehl (1963)
Tritium perpendicular and parallel to c-axis in natural single crystals. Diffusion time of 7 days.	2.45×10^{-15}	0.67 ± 0.09	Itagaki (1964)
Tritium parallel to c-axis in natural single crystals. Diffusion time greater than 2 days.	2.12×10^{-15}	0.54 ± 0.09	Itagaki (1966, 1967)
Tritium perpendicular to c-axis in natural single crystals. Diffusion time greater than 2 days.	2.42×10^{-15}	0.65 ± 0.05	Itagaki (1966, 1967)
Tritium parallel to c-axis in artificial single crystals.	2.15×10^{-15}	0.63 ± 0.03	Blicks et al. (1966)
Tritium perpendicular to c-axis in artificial single crystals.	2.40×10^{-15}	0.63 ± 0.03	Blicks et al. (1966)
Oxygen-18 in artificial single crystals.	3.1×10^{-15}	0.68 ± 0.13	Delibaltas et al. (1966)
Tritium parallel to c-axis in artificial single crystals.	2.5×10^{-15}	0.63 ± 0.05	Dengel et al. (1966)
Tritium parallel to c-axis in artificial single crystals.	1.44×10^{-15}	0.62 ± 0.03	Ramseier (1967)
Tritium perpendicular to c-axis in artificial single crystals.	1.68×10^{-15}	0.62 ± 0.07	Ramseier (1967)
Tritium parallel to c-axis in natural single crystals.	1.54×10^{-15}	0.61 ± 0.02	Ramseier (1967)
Tritium perpendicular to c-axis in natural single crystals.	1.65×10^{-15}	0.62 ± 0.04	Ramseier (1967)

Consider what happens in the crystal during rapid cooling. The term "rapid" means that the cooling takes place during a period much less than that required for the new equilibrium defect concentrations to be established. When the temperature is lowered, equal numbers of vacancies and interstitials disappear rapidly owing to their mutual annihilation. Then some fraction of defects that are predominant must "die" in a slower and more difficult way—for instance, by diffusing towards the surface or concentrating into disk clusters, as shown in Figure 3. The edges of these disks are edge dislocation loops, with the Burgers vector normal to the plane of the disk. If loops of a-type are predominant, then the major defects are vacancies; if loops of b-type are predominant, then the major defects are interstitials.

Dislocation loops (Fig. 4) can expand or contract because of diffusion of point defects toward (or from) the loops, caused by a change in temperature or applied pressure. Monitoring the growth or contraction of dislocation loops by means of X-ray topography in ice monocrystals, Higashi and Hondoh with co-authors determined the diffusion coefficient of interstitials in ice D_i, the formation energy of interstitials E_{as}, the activation energy of their motion U_{im}, the activation volumes of interstitials V_{if} and of their migration V_{im}, and absolute values of the interstitial concentration n_i, and the entropy S_v/k_B. Table 3 contains all of these data.

According to these results, the activation energy of self-diffusion in ice $E_s = E_{as} + E_{im} = 0.56$ eV, and the absolute value of the self-diffusion coefficient is in good agreement with results obtained

Figure 2. Comparison of the self-diffusion coefficients D in ice obtained by the tracer technique (^{3}H and ^{18}O) and calculated from the diffusion coefficients of self-interstitials obtained by the X-ray topography (solid line) (after Oguro et al. 1988).
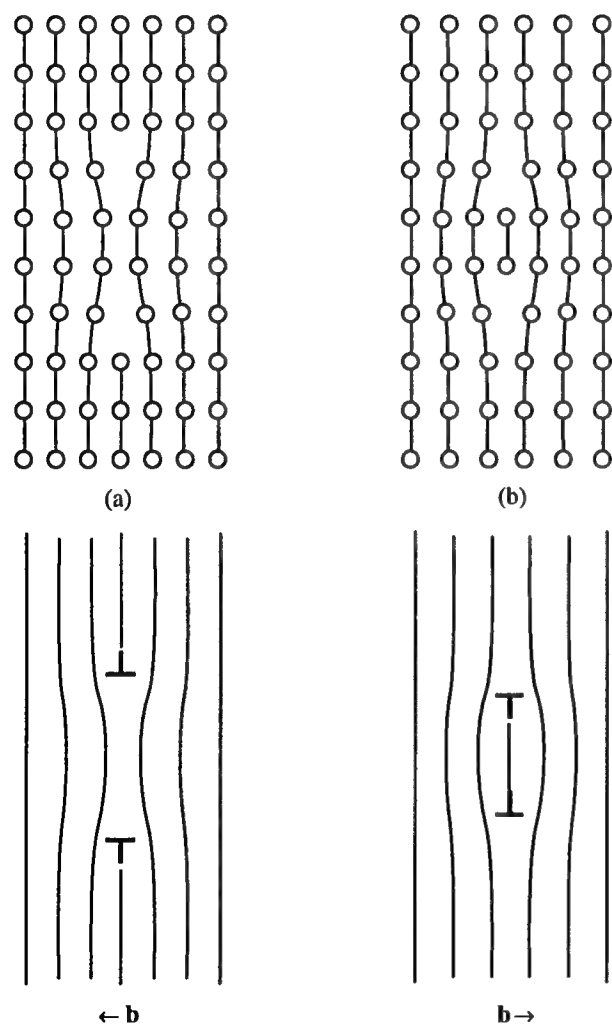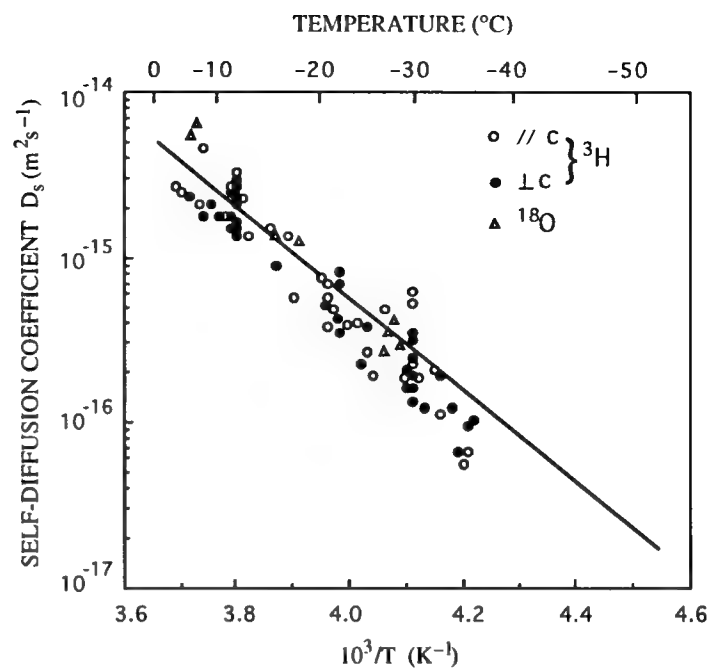

(a) (b)

Figure 3. Two types of the prismatic dislocation loop— (a) vacancy type and (b) interstitial type. Schematic atomic arrangement at the top corresponds to edge dislocation loops of different signs (after Oguro et al. 1988).

← b b →

6

Table 3. Self-diffusion interstitial parameters in ice at 0°C (after Hondoh 1992). V_{mol} is a molecular volume in ice ($V_{mol} \approx 3.3 \times 10^{-23}$ cm³).

n_i/N	E_{as} (eV)	S_v/k_B	D_i (m²/s)	U_{im} (eV)	V_{if}/V_{mol}	V_{im}/V_{mol}
2.8×10^{-6}	0.40	4.9	2×10^{-9}	0.16	−0.26	0.40

earlier by the radioactive tracer technique (Fig. 2). We refer readers interested in the details of an elegant experimental technique, employed by Higashi and Hondoh et al., to their review papers (Hondoh et al. 1987, Oguro et al. 1988, Hondoh 1992), where one can find references to their original papers.

Thus, from measurements of self-diffusion in ice it is not possible to determine any of the characteristics of vacancies, since the predominant defects are interstitials (at least at $T \geq -50°C$). The only studies in which activation parameters of vacancies in ice were possibly determined were those in which a positron annihilation technique was used (Mogensen and Eldrup 1978, Eldrup and Morgensen 1978). When ice is exposed to positrons, thermalized positrons and positronium atoms (electron + positron) are captured mainly by vacancies. Therefore, their lifetimes depend on the concentration and mobility of vacancies. It is extremely difficult to estimate the absolute accuracy of this method since it is based on a considerable number of assumptions and approximations. The vacancy migration energy found in these papers was 0.34 ± 0.07 eV and its formation energy was found to be between 0.2 and 0.35 eV.

PROTONIC DEFECTS

As explained in the earlier reports on the *Structure of Ordinary Ice I_h; Part I: Ideal Structure of Ice* and *Electrical Properties of Ice* (Petrenko 1993a,b), many important properties arise from the disorder of the protons in the structure. This allows molecules to rotate, giving rise, for example, to dielectric polarization, but such rotations cannot occur without the aid of special kinds of point defects in the protonic subsystem. The structure of ice is shown in Figure 4a. There are two possible positions for protons on each bond, but in the perfect structure the occupation of these sites is governed by the so-called Bernal-Fowler rules or simply the "ice rules":

1. Two protons are located near each oxygen atom.
2. There is one proton per hydrogen bond.
The first rule ensures electroneutrality of the water molecules, and the second ensures the perfection of the hydrogen bonds. Violations of these rules at particular bonds or molecules result in the formation of the four protonic defects shown in Figure 4b. These are the H_3O^+ and OH^- ions and the Bjerrum L- and D-defects, which are bonds with no protons or two protons respectively (Bjerrum 1951). An ion moves from one site to another merely by the transfer of a proton from one end of a bond to another, and a Bjerrum defect moves by the rotation of a water molecule.

The structure of the hydrogen bonds, along which the protons move, constitutes a three-dimensional grid. The transfer along this grid of any of the above defects reorients water molecules in such a fashion that a second defect of the same type cannot pass along the same path in the same direction.

To better understand what happens in the process of ionic and Bjerrum defect transfer, let us consider the track of an arbitrary charge carrier, a positive H_3O^+ ion, for instance. When we are speaking about ionic or Bjerrum defect transfer, it is important to realize that oxygen atoms do not "hop" from one lattice site to the next one. Only protons move, with a subsequent redistribution of the electronic density on the neighboring molecules. Thus, when speaking about H_3O^+ motion, we have in mind that a characteristic distribution of three protons near an oxygen atom shifts in space.

When a proton jumps along a hydrogen bond from one water molecule to another, a pair of H_3O^+ and OH^- ions is produced, as shown in Figure 4b. Formation of this ion pair and further separation of the ions require considerable energy of about 1 eV (see the review of experimental results in Petrenko 1993a). After an ion is formed, it can migrate from one site to another through proton jumping along hydrogen bonds. This pro-

a. Defect free structure of ice I$_h$.
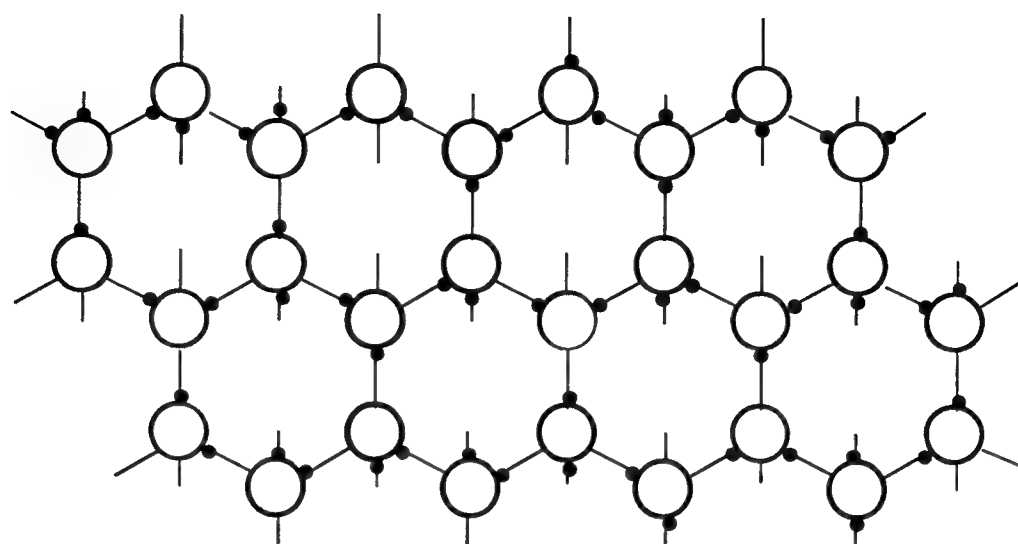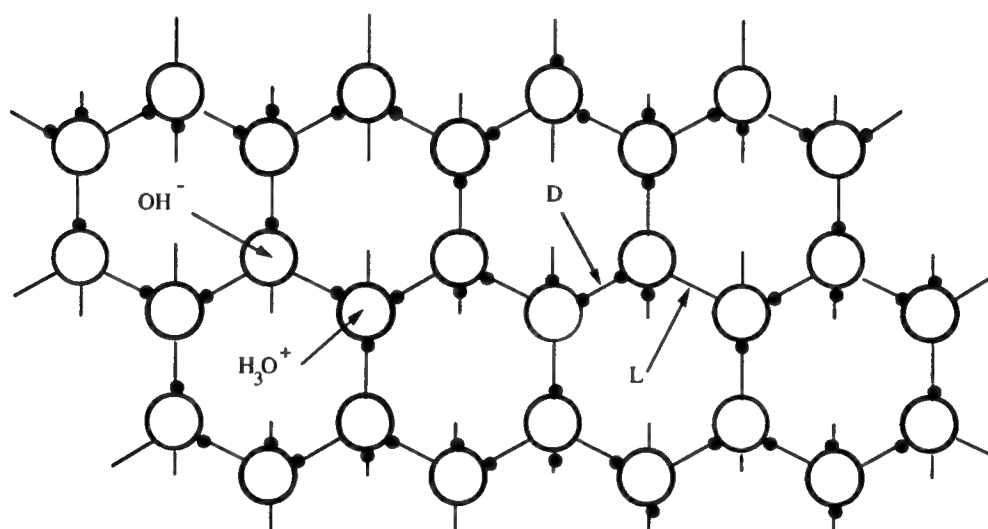
b. Ice with H$_3$O$^+$ and OH$^-$ ions and D- and L-defects.

Figure 4. Ice structures.

cess is illustrated schematically for the straightened out chain of molecules shown in Figures 5a and b.

When a proton jumps from one bond to another, two neighboring defective hydrogen bonds are produced. These are the so-called D- and L-defects. Since a proton has a positive electrical charge, it is not difficult to see that a D-defect is positively charged and an L-defect is negatively charged. Formation and separation of a pair of Bjerrum defects require energy of 0.68 eV. Already formed L- and D-defects can migrate in the ice lattice by protons jumping between neighboring hydrogen bonds as illustrated for a D-defect in Figures 5c and d.

An H$_3$O$^+$ ion migrates from left to right along a water molecule chain by consecutive jumps of protons along hydrogen bonds. Therefore, if in the beginning the protons on all bonds in the chain were located in the left-hand positions (Fig. 5a), after an H$_3$O$^+$ ion has passed, all protons will be in the right-hand positions. This path is now closed for proton transfer in the same direction. The reader can easily make sure that the migration of an OH$^-$ ion from right to the left would result in exactly the same rearrangement of this molecular

8
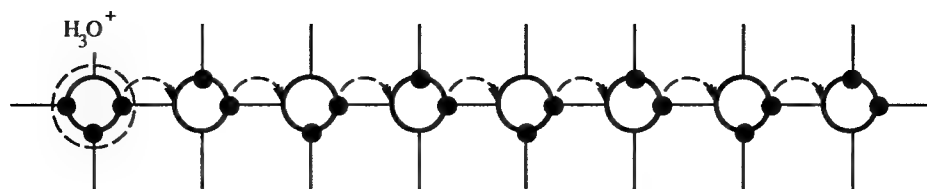
a. Initial arrangement of H_3O^+ ion and water molecules in the chain before the ion moves from the left to the right. The arrows indicate successive proton hops (along the bonds) by means of which the ion moves.
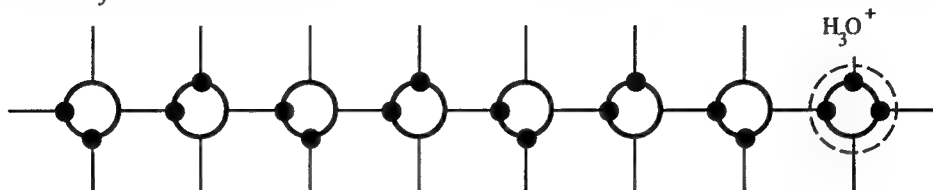
b. Chain after the ion has passed. Obviously, no further H_3O^+ ion can go along the same chain in the same direction.
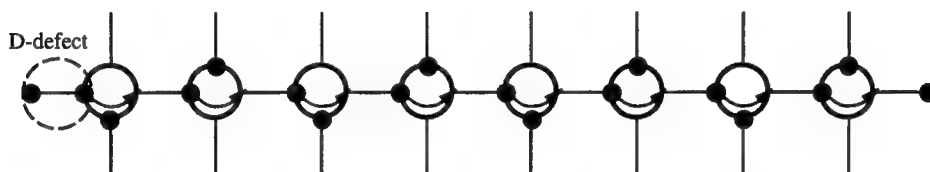
c. D-defect motion from left to right along the chain as in Figure 5b. The arrows indicate successive hops of protons from one bond to next one.
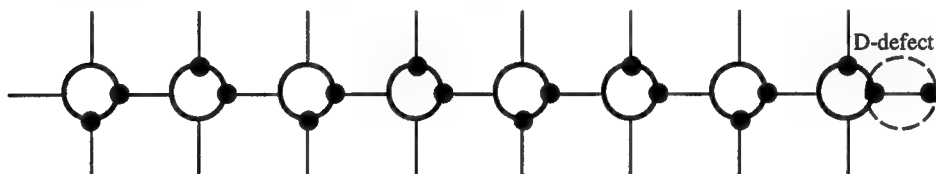
d. Chain after the D-defect has passed. Comparison with Figure 5a shows that motion of D-defect restored positions of the protons along the chain. It is ready (or "open") now for the passage of another H_3O^+ ion.

Figure 5. Schematic representation of H_3O^+ ion (a, b) and D-defect (c, d) motion along a chain of hydrogen bonds in ice.

chain. Since H_3O^+ and OH^- ions drift in opposite directions in an external electric field, we come to the conclusion that both types of ions drifting in a given field "block" molecular tracks in the same manner.

If we now consider the migration in the same field of a positively charged D-defect along the same chain (Fig. 5c) "blocked" by an H_3O^+ ion passing along it, it turns out that the D-defect "unblocks" the chain, restoring the initial configuration to that of Figure 5d, which is the same as Figure 5a. In the same fashion the migration of a

negatively charged L-defect "unblocks" the chain if it migrates from right to left.

Ions and Bjerrum defects migrating through ice reorient water molecules, altering conditions for their transfer. One can say that in ice protonic defects interact in a very special way: via those changes in the molecule configuration that they produce during their transfer. In addition the more usual interactions between defects also take place. First, protonic defects are electrically charged, which results in a strong Coulomb interaction, and second, as we shall see later (in the *Activation*

Volume of Protonic Defects section), the presence of a defect introduces a lattice deformation that can lead to interactions via elastic stresses.

In thermal equilibrium, which is characterized by maximum entropy S, water molecules are oriented randomly, subject to the ice rules. Any flux of defects of the same type (H_3O^+ ions, for example) $\vec{j}_1$ will increase the number of molecules oriented along the direction of the flux. The new configuration of water molecules is more ordered and therefore has smaller entropy. These ideas were formulated mathematically by Jaccard (1959, 1964) and independently by Onsager and Depuis (1960). They introduced the configurational vector $\vec{\Omega}$, describing changes occurring in ice because of protonic defect transfer. If at time $t = 0$ ice is unpolarized and in thermal equilibrium, then

$$\vec{\Omega} = \int_0^t \left(\vec{j}_1 - \vec{j}_2 - \vec{j}_3 + \vec{j}_4 \right) dt \tag{23}$$

where $\vec{j}_i$ ($i = 1,2,3,4$) denote the fluxes of H_3O^+, OH^- and D- and L-defects respectively. This notation of protonic defects is generally accepted and we shall use it hereafter. If we introduce the quantities η_i given by

$$\eta_i = 1,-1,-1,1 \text{ for } i = 1,2,3,4, \tag{24}$$

then eq 23 can be simplified to

$$\vec{\Omega} = \sum_{i=1}^{4} \int_0^t (\eta_i \vec{j}_i \, dt) \,. \tag{25}$$

The choice of + or – before $\vec{j}_i$ in eq 23 accounts for different effects produced by defects on the reorientation of water molecules. Thus, for example, as we have seen in Figure 5, the effect of an H_3O^+ ion ($i = 1$) is opposite to the effect of a D-defect ($i = 3$).

Configurational entropy S_c must somehow be related to $\vec{\Omega}$. For small decrements of entropy we can use the first term of a Taylor series

$$\Delta S_c \propto -\Omega^2 \,. \tag{26}$$

There is no linear term because ΔS_c cannot depend on the sign of the fluxes producing it. For the time derivative of the entropy we have

$$\dot{S} \propto -\vec{\Omega} \, \dot{\vec{\Omega}} \,. \tag{27}$$

The proportionality factor in eq 27, which we denote as Φ/T, can in principle be both calculated theoretically and determined experimentally. Attempts to calculate Φ theoretically (Jaccard 1959, 1964; Hubmann 1979a,b) yield only the right order of magnitude of this quantity, and the most reliable value is that found in an analysis of experimental data by Hubmann (1979a)

$$\frac{\Phi}{T} = 3.85 \; k_B r_{oo} \tag{28}$$

where $r_{oo} = 2.76$ Å is the oxygen–oxygen distance in ice.

According to Ryzhkin* the difference between the theoretical and experimental values of Φ/T is caused by taking into account reorientation of molecules, not only in this water molecule chain, but also reorientation of neighboring molecules when considering a defect transfer along a chain. However, such calculations are quite cumbersome and have not been made yet. Accordingly, we shall use the value of Φ found experimentally.

Charge carriers in ordinary ice I_h are, under usual conditions, one of these four types of protonic defects. A detailed discussion on the nature of electric charges in ice can be found in the report by Petrenko (1993a). "Usual conditions" are understood here as an absence of excitation by direct ultraviolet light, electron beams, γ rays, etc.

The electric current density $\vec{J}$ in ice can now be written

$$\vec{J} = \sum_{i=1}^{4} e_i \vec{j}_i \tag{29}$$

where e_i are the effective charges carried by the defects. Since H_3O^+ and OH^- ions and L- and D-defects are created and annihilated in pairs, it is obvious that

$$e_1 = -e_2 \text{ and } e_3 = -e_4 \,. \tag{30}$$

If we place an extra "foreign" proton into an otherwise normal ice lattice, we will inevitably produce two carriers at once: an H_3O^+ ion and a D-defect, as shown in Figure 6. Hence, the sum of these charges equals a proton charge e

$$e_1 + e_3 = e \,. \tag{31}$$

*Personal communication with Dr. Ivan Ryzhkin during the International Symposium on Physics and Chemistry of Ice, September 1991, Sapporo, Japan.
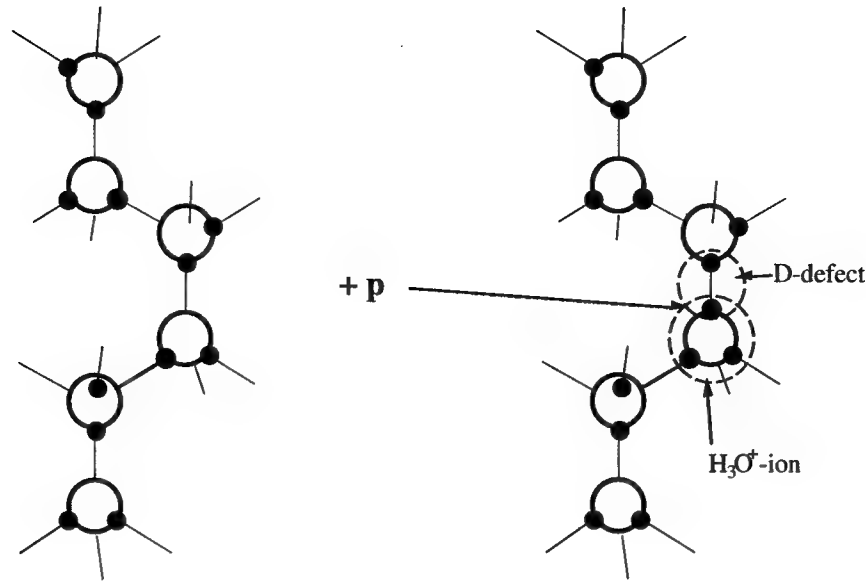
Figure 6. Creation of two point defects (H_3O^+ ion and D-defect) when a proton is placed into defect-free ice lattice.

To find out how the elementary protonic charge is shared between the ion and the D-defect, we must consider both the fraction of the intermolecular distance that the proton travels in the case of ionic or Bjerrum defect transfer and the associated displacement of electronic charge density when the defect moves along the chain.

The most strict theoretical analysis of this problem was conducted by Scheiner and Nagle (1983) who found

$$e_3 = (0.36 \pm 0.03)e. \tag{32}$$

The other way to find e_1 and e_3 is by experiment. In ice the charge of the predominant defect is incorporated in the formula for static dielectric permittivity ε_s (see Petrenko 1993a). Using this fact and analysis of experimental data of measurements of ε_s for specially doped ices (in such a fashion that either ions or Bjerrum defects predominated), Hubmann (1979a,b) found

$$e_3 = (0.38 \pm 0.01)e \tag{33}$$

which is remarkably close to the calculations of Scheiner and Nagle. Other recent experimental results for e_1 and e_3 are given in Table 4. These results are close to those represented in eq 32 and 33.

The rate of heat generation in a unit volume $\dot{Q}$ by current flowing through ice is determined by two effects. The first is simply the Joule heat $\vec{E}\vec{J}$, and the second is the change in the configurational entropy $T\dot{S}_c$ Accordingly

$$\dot{Q} = \vec{E}\vec{J} - \Phi \vec{\Omega} \dot{\vec{\Omega}}. \tag{34}$$

Using eq 25 and 29 we obtain

$$\dot{Q} = \sum_{i=1}^{4} \left(e_i \vec{E} - \eta_i \Phi \vec{\Omega} \right) \vec{j}_i. \tag{35}$$

As can be seen from eq 35, the effective force acting upon charge carriers in ice consists of two terms, as opposed to ordinary conductors

Table 4. Ratios of effective electric charge of H_3O^+ ion (e_1) and of D-defect (e_3) to proton charge (e).

e_1/e	e_3/e	Reference
0.61 ± 0.02	0.39 ± 0.01	Zaretskii et al. (1988)
0.62 ± 0.01	0.38 ± 0.01	Hubmann (1979a)
0.626	0.374	Takei and Maeno (1987)
0.64 ± 0.03	0.36 ± 0.03	Scheiner and Nagle (1983)

$$\vec{F}_i = e_i \vec{E} - \eta_i \Phi \vec{\Omega}. \tag{36}$$

Accordingly, for the charge carrier fluxes we have

$$\vec{j}_i = \left(e_i \vec{E} - \eta_i \Phi \vec{\Omega} \right) n_i \mu_i / e_i \tag{37}$$

where μ_i is the mobility (i.e., velocity per unit electric field) of defect i. If the distribution of protonic defects in ice is not uniform, we have to add the diffusion flux to eq 37, giving

$$\vec{j}_i = \left(e_i \vec{E} - \eta_i \Phi \vec{\Omega} \right) n_i \mu_i / e_i - D_i \,\mathrm{grad}\, n_i \tag{38}$$

in which the diffusion coefficient D_i is equal to $k_B T \mu_i / |e_i|$. The four equations (eq 38, $i = 1, 2, 3, 4$) are the most general equations describing charge carrier transfer in ice and can account for all electrical properties of ice known today (Petrenko 1993a).

Statistics of protonic point defects in ice

To calculate the equilibrium concentration of protonic point defects, we can follow the same general procedure that was described in the *General Consideration of Point Defects* section. For ice with ionic defects, such a calculation was made by Ryzhkin (1985), who carefully calculated the entropy of ice with H_3O^+ and OH^- ions. Minimizing the free energy F, Ryzhkin then obtained for the equilibrium concentration of ions

$$\frac{n_i}{N - 2n_i} = \frac{2}{3} \exp\left(-\frac{E_{ai}}{2k_B T}\right) \tag{39}$$

where E_{ai} is the formation energy of a pair of ions, and since $E_{ai} \gg 2k_B T$

$$n_i \approx \frac{2}{3} N \exp\left(-\frac{E_{ai}}{2k_B T}\right). \tag{40}$$

As we can see, the specific structure of ice manifested itself only in the appearance in eq 40 of a factor of 2/3 before the exponent. We can interpret this factor in simple terms as the ratio of the number of possible orientations of an ion (four available) to the number of possible orientations of a water molecule (which is six). The factor 1/2 is in the exponent because ions are created in pairs.

The general case of the presence of ions and Bjerrum defects was also considered by Ryzhkin (unpublished data, 1985). Let us denote the D-defect concentration as n_D and the concentration of L-defects as n_L. If D- and L-defects are formed by thermal fluctuations, i.e., in pairs, then obviously

$$n_D = n_L. \tag{41}$$

Using a method similar to the one seen above, Ryzhkin found that in the presence of both types of defects

$$S/(k_B N) = -2\,x\,\ln(x) - (1-2\,x)\,\ln(2\,(1-2\,x)/3)$$
$$- 4\,y\,\ln(2\,y) - 2\,(1-2\,y)\,\ln(1-2\,y) \tag{42}$$

where

$$x = n_i/N \text{ and } y = n_D/N. \tag{43}$$

Minimizing the free energy of ice with the entropy from eq 42, we obtain for the Bjerrum defect concentration

$$n_D = n_L = n_{H_2O} \exp\left(-\frac{E_{aB}}{2k_B T}\right). \tag{44}$$

Protonic defects can also be introduced into ice by doping with certain impurities. This case will be considered in the *Impurities* section.

Electrical properties of protonic defects

As we have indicated previously, protonic defects are charge carriers in ice and hence determine its electrical properties. A detailed description of the electrical properties of ice and experimental techniques for their investigation can be found in the recent review by Petrenko (1993a). Here, we shall only point out what information concerning protonic defects can be obtained from analysis of the electrical properties of ice.

When an alternating electric field with angular frequency ω is applied to ice, in addition to the drift current (eq 29), $\vec{J}_{dr}$, we have to add the displacement current $\vec{J}_{dis}$, so that the total current is

$$\vec{J} = \vec{J}_{dis} + \vec{J}_{dr} \tag{45}$$

$$\vec{J}_{dis} = \varepsilon_0 \varepsilon_\infty \frac{\partial \vec{E}}{\partial t} \tag{46}$$

where ε_0 is the dielectric permittivity of free space and ε_∞ is the high-frequency dielectric permittivity of ice arising from its electronic polarizability; $\varepsilon_\infty \approx 3.2$.

A complete description of the electrical properties of ice, i.e., its electrical conductivity $\sigma(\omega)$ and dielectric permittivity $\varepsilon(\omega)$, can be found in the system of eq 25, 29, 45 and 46 (see Petrenko 1993a, for instance). In the absence of interfaces and concentration gradients, the answer can be expressed

as follows

$$\sigma(\omega) = \sigma_s + \frac{(\sigma_\infty - \sigma_s)(\omega \, \tau_D)^2}{1 + (\omega \, \tau_D)^2} \qquad (47)$$

$$\varepsilon(\omega) = \varepsilon_\infty + \frac{\varepsilon_s - \varepsilon_\infty}{1 + (\omega \, \tau_D)^2} . \qquad (48)$$

Here, we have introduced new terms

$$\sigma_\infty = \sum_{i=1}^{4} \sigma_i \text{ with } \sigma_i = n_i |e_i| \, \mu_i \qquad (49)$$

$$e^2/\sigma_s = \frac{e_1^2}{\sigma_1 + \sigma_2} + \frac{e_3^2}{\sigma_3 + \sigma_4} \qquad (50)$$

$$\tau_D^{-1} = \omega_D = \Phi \left[\frac{\sigma_1 + \sigma_2}{e_1^2} + \frac{\sigma_3 + \sigma_4}{e_3^2} \right] \qquad (51)$$

$$\varepsilon_s = \varepsilon_\infty + \frac{1}{\varepsilon_0 \Phi} \frac{\left(\dfrac{\sigma_1 + \sigma_2}{e_1} - \dfrac{\sigma_3 + \sigma_4}{e_3} \right)^2}{\left(\dfrac{\sigma_1 + \sigma_2}{e_1^2} + \dfrac{\sigma_3 + \sigma_4}{e_3^2} \right)^2} . \qquad (52)$$

By varying the temperature or the type and concentration of dopants, or both (see the *Impurities* section), any one of the four σ_i terms can be made dominant. Then eq 52 is simplified to yield

$$\varepsilon_s \approx \varepsilon_\infty + \frac{e_i^2}{\varepsilon_0 \, \Phi} . \qquad (53)$$

Measurements of ε_s for doped ice in which ionic defects and Bjerrum defects dominate the electrical properties thus permit both the charges e_i and Φ to be determined. This is the basis of the results quoted in Table 4.

As we can see from eq 49 and 50, σ_∞ is determined by the largest σ_i, and σ_s is determined by the lower of $(\sigma_1 + \sigma_2)$ and $(\sigma_3 + \sigma_4)$. In pure monocrystalline ice $(\sigma_3 + \sigma_4) \gg (\sigma_1 + \sigma_2)$ and $\sigma_4 \gg \sigma_3$. Consequently, the measurement of σ_∞ as a function of temperature allows us to determine the activation energy of the partial conductivity σ_4 of L-defects, $E_{\sigma 4}$

$$\sigma_\infty \approx \sigma_4 = \sigma_{40} \exp \left(- \frac{E_{\sigma 4}}{k_B T} \right). \qquad (54)$$

Since the conductivity of Bjerrum defects greatly exceeds (usually by two or three orders of magnitude) the ionic conductivity, and the mobility of H_3O^+ ions exceeds the mobility of OH^- ions, we have

$$\sigma_s \approx \left(\frac{e}{e_1} \right)^2 \sigma_1 \qquad (55)$$

Therefore, from the temperature dependence $\sigma_s(T)$, it is possible to calculate the conductance activation energy $E_{\sigma 1}$ of H_3O^+ ions. Since conductivities are the products of concentrations and mobilities, the activation energies $E_{\sigma i}$ obtained are, generally speaking, the sums of formation energies $(E_{ai}/2)$ and activation energies of migration of these defects E_{mi}. To separate out $(E_{ai}/2)$ and E_{mi}, usually a known concentration of specific defects is achieved by some technique and then the σ_i are measured. The known concentration of the defects can be created with proton injection (Petrenko et al. 1983), a field effect transistor (Petrenko and Maeno 1987) or with doping of ice (see the *Impurities* section). Thus, in many cases it is possible to determine separately concentrations n_i and mobilities μ_i of protonic defects.

The most well-established conductivity parameters of pure monocrystalline ice are the high-frequency conductivity σ_∞ and its activation energy $E_{\sigma\infty}$. For $T > -50°C$ these depend only on the L-defects. These quantities can be well reproduced because, first, high-frequency measurements do not depend upon the type of electrode used and, second, because of the comparative ease with which specimens can be obtained that are pure enough for the L-defect concentration to be intrinsic. The same holds for τ_D and its activation energy E_τ, since according to eq 49–51, $\tau_D^{-1} \propto \sigma_\infty$ when $\sigma_\infty \gg \sigma_s$ (i.e., when the majority type of charge carrier is clearly distinguished). These four values at $T = -10°C$ are as follows

$$\begin{aligned}
E_{\sigma\infty} &= (0.58 \pm 0.03)\text{eV} \\
E_\tau &= (0.58 \pm 0.01)\text{eV} \\
\sigma_\infty &= (1.8 \pm 0.2)10^{-5} \, \Omega^{-1} \, m^{-1} \\
\tau_D &\approx 5 \times 10^{-5} \, s .
\end{aligned} \qquad (56)$$

The Debye dispersion shown in Figure 7 is reproduced very well in good quality single crystals: pure, homogeneous and annealed (for relaxation of internal stresses).

Much greater scatter is observed in measurements of the static conductivity σ_s of undoped ice and its activation energy E_{σ_s}. Values of E_{σ_s} have been found to lie between 0 and 0.7 eV and σ_s $(-10°C)$ varies from 10^{-6} down to $6 \times 10^{-10} \, \Omega^{-1}$ m^{-1}. This variation is explained by the difficulty of purifying ice to a level at which intrinsic ions dominate over ions supplied by impurities. That is why von Hippel et al. (1973) concluded that there
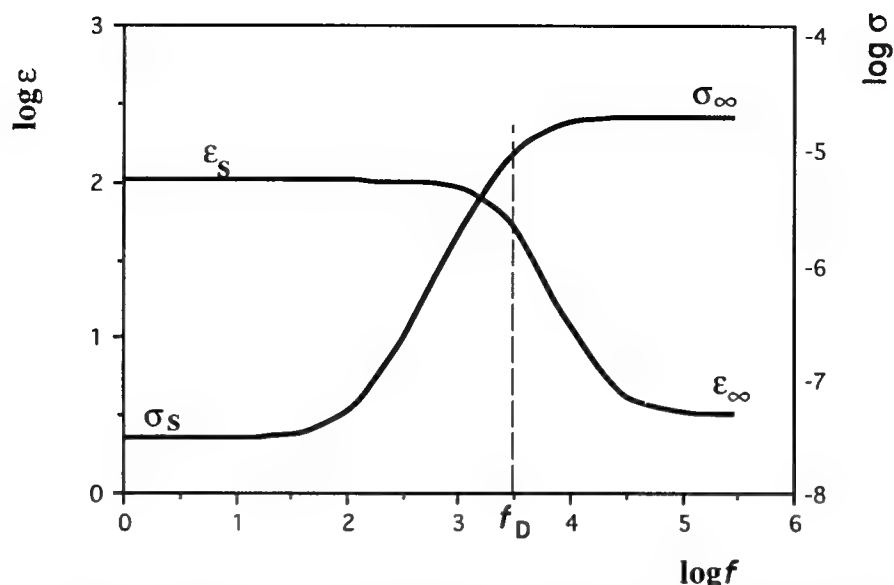
13

Figure 7. Typical frequency dependence of permittivity ε and of conductivity σ of pure single crystalline ice at $T = -10C°$ *(after Petrenko 1993a).*

are no intrinsic ions in ice and that all ions originate from impurities. If we refer to Table I of their paper (von Hippel et al. 1971) for the value of σ_s $(2.5 \times 10^{-8} \ \Omega^{-1} \ m^{-1})$ and compare it with the minimum observed value of $6.4 \times 10^{-10} \ \Omega^{-1} \ m^{-1}$, then we might agree with them that their ions were of impurity origin. The question, however, remains open: were the specimens in the experiments of Wörz and Cole (1969) or Petrenko et al. (1983) pure enough that their conductivity may be considered intrinsic? We observed the following general trend: the purer the ice is, the smaller is σ_s and the greater is E_{as}. Therefore, the value of the activation energy of creation of an ion pair $E_{ai} =$ 0.96 eV (Eigen and De Maeyer 1956, 1957, 1958; Eigen et al. 1964), for a long time accepted as the true value, should be treated as the lowest possible limit of this quantity. As the current upper limit we have $E_{ai} = 2E_{\sigma_s} = 1.4$ eV from the work of Petrenko et al. (1983). The above discussion implies that ion mobility almost does not depend on temperature, that is, the ion motion is not a thermoactivated process. That suggestion was proven by experiment (see, e.g., Kunst and Warman 1983).

The determination of charge carrier mobilities in ice is an extremely difficult task, since, because of small values of μ_i and the "jump" mechanism of motion, the regular technique for measuring the Hall effect is not applicable in this case. (The Hall effect is discussed in the future report on the

Surface of Ice.) Hopes of using "saturation currents" for determining μ_i are not justified because of reasons pointed out by Maidique et al. (1971) in their critique of Eigen's work, and also because when high voltage is applied to a system with ice/metal interfaces, various physical phenomena are observed that make the interpretation of results more complicated (see Part II of Petrenko 1993a).

Nonetheless, several new techniques for determining charge carrier mobilities in ice have been developed and employed during the last 25 years. These are: the technique that measures stationary and transient injection currents (Eckener et al. 1973, Petrenko et al. 1983, Petrenko and Ryzhkin 1984b); the ice field effect transistor (Petrenko and Maeno 1987); and the technique that measures low-frequency dispersion (Petrenko and Ryzhkin 1984a, Zaretskii et al. 1988, Zaretskii 1991). The idea of determining μ_i and n_i from the parameters of low-frequency dispersions was presented by Petrenko (1993a). Other techniques mentioned above are described and discussed in Part II of the same review. The results of determining charge carrier mobilities in ice are summarized in Table 5. At first glance only the data on L-defect mobilities seem to be satisfactory. At $T = -10°C$, $\mu_4 \approx (2-5) \times 10^{-8} \ m^2 \ V^{-1} \ s^{-1}$. This mobility drops exponentially with decreasing temperature, the activation energy being $0.19 - 0.235$ eV (see Table 6). There is still no reliable information about D-defect mobil-

Table 5. Mobilities of charge carriers in ice.

T (°C)	H_3O^+ μ_1 (m²/V s)	OH^- μ_2 (m²/V s)	D μ_3 (m²/V s)	L μ_4 (m²/V s)	Method used	Reference
−13...−36	$(1.1 \pm 0.1) \times 10^{-7}$	...	—	—	Analysis of conductivity decay	Kunst and Warman (1983)
−10	2.5×10^{-8}	—	—	—	σ_s and E_{as} measurements	Wörz and Cole (1969)
0... −20	5×10^{-7}	—	—	—	Saturation currents	Maidique et al. (1970)
−123	—	$\leq 4 \times 10^{-7}$	—	—	Doping with KOH	Zaretskii et al. (1988)
−5... −40	$10^{-9} - 10^{-7}$	—	—	—	Proton injection	Petrenko et al. (1983)
0	2.7×10^{-8}	—	—	5×10^{-8}	Doping with HF	Camplin et al. (1978)
−10	—	—	—	1.8×10^{-8}	Doping with HF	Jaccard (1959)
—	—	$\geq 2 \times 10^{-10}$	—	—	Doping with KOH	Howe and Whitworth (1989)
−10	$(2.4 \pm 1.6) \times 10^{-7}$	—	—	—	Saturation currents	Bullemer et al. (1969)
−10	3.5×10^{-8}	—	—	—	HF doping	Camplin and Glen (1973)
−33.1	9.2×10^{-8}	2.7×10^{-8}	—	—	Ice field effect transistor	Petrenko and Maeno (1987)
−145... −178	$(9 \pm 1) \times 10^{-8}$	—	—	—	Transient injection of protons	Eckener et al. (1973)
−10	$\approx 10^{-6}$	—	—	1.7×10^{-8}	Low-frequency dispersions	Zaretskii et al. (1987a)
−33	$(6.7 \pm 0.8) \times 10^{-7}$	—	—	—	Low-frequency dispersions	Zaretskii (1991)
−20	6×10^{-8}	—	—	—	Proton injection	Petrenko and Ryzhkin (1984c)
−10	—	2.4×10^{-8}	—	—	Recombination injection	Petrenko and Chesnakov (1990c)
−10	$(9 \pm 3) \times 10^{-8}$	7×10^{-9}	—	—	Analysis of data	Chen et al. (1974)

ity. There are only indirect evidences that $\mu_3 < \mu_4$. For example, Devlin (1992), citing spectroscopic data, indicated that, in the region at 150 K, μ_3 is orders of magnitude less than μ_4.

Data on ionic mobilities are distinguished at first glance by their large scatter (from 5×10^{-7} down to 2.5×10^{-8} for H_3O^+ and from 4×10^{-7} down to 2×10^{-10} for OH^-). However, if we discard the large values obtained by the now-discredited method of saturation currents and the values obtained from measurements of low-frequency dispersions (which still have low accuracy), it appears that the positive ion mobility lies within the limits of 2.7×10^{-8} and 1.1×10^{-7} m²/V s—not bad at all! The authors of this review prefer the data obtained in transient injection experiments (Eckener et al. 1973), in which a minimum of assumptions was used. The same H_3O^+ ion mobility was found by Petrenko and Maeno (1987) using field effect transistors. So it is likely that $\mu_1 \approx 10^{-7}$ m² V⁻¹ s⁻¹. It seems well established that both H_3O^+ and OH^- ions move in ice with zero activation energy.

Concluding this section about point defects' mobilities, we can now explain the at first slightly surprising fact that the self-diffusion coefficients of oxygen and hydrogen in ice are equal (Table 2). This is unexpected because the oxygen can diffuse only as a part of a water molecule, whereas the hydrogens can also move by ion and Bjerrum defect migration. Let us compare the absolute values of diffusion coefficients of hydrogen in these two processes. If the hydrogens diffuse in ice by protonic defect transfer, then the diffusion coefficient D_H is

$$D_H = \frac{n_1 D_1 + n_2 D_2}{n_{H_2O}} \tag{57}$$

where $n_{1,2}$ and $D_{1,2}$ denote the concentrations and diffusion coefficients of those protonic defects that limit the transfer of protons over macroscopic distances. In pure ice these defects are ions. Therefore, we can rewrite eq 57 in the form

$$D_H \approx \frac{e_1(n_1\mu_1 + n_2\mu_2)k_BT}{e_1^2 n_{H_2O}} \approx \frac{\sigma_s \cdot k_BT}{e^2 \cdot n_{H_2O}} \tag{58}$$

where σ_s is the static electric conductivity of ice.

For D_H to exceed the self-diffusion coefficient D_s, the following inequality must hold

$$\sigma_s \geq D_s \frac{e^2 n_{H_2O}}{k_B T} \approx 3.9 \times 10^{-4} \ (\Omega \ m)^{-1} . \quad (59)$$

In eq 59 we have used $D_s \approx 2 \times 10^{-15}$ m^2 s^{-1} ($T = -10°C$) from Table 2. Since in pure ice at $-10°C$ $\sigma_s \leq 10^{-8}$ $(\Omega m)^{-1}$ (Petrenko 1993a), the diffusion rate of hydrogen in ice is faster when it diffuses as a part of a water molecule in the form of an interstitial. That explains the equality of the diffusion coefficients of hydrogen and oxygen. However, in ice heavily doped with HF or KOH, σ_s would be sufficiently large for hydrogen transfer by protonic defects to be faster than that by interstitial diffusion of H_2O molecules. There are no experimental data on self-diffusion coefficients in doped ice.

Activation volume of protonic defects

The formation of any protonic point defect results in deformation of the surrounding lattice. In the case of Bjerrum defects, the defective hydrogen bonds are weaker than the normal ones, and therefore they will be longer. This is obvious in particular for a D-defect, where there exists an extremely strong repulsion between two protons on one hydrogen bond. Accordingly, one can assume that Bjerrum defects "expand" ice, increasing its volume. If ice is under pressure P then the formation energy of the ith defect E_{ai} is increased by the amount of work against this pressure

$$E_{ai}(P) = E_{ai}(0) + P\gamma_{ai} \quad (60)$$

where γ_{ai} is the so-called activation volume. For the defects that increase volume, γ_{ai} is positive and their formation energy is raised proportionally to the applied pressure. This results in an exponentially decreasing concentration of such defects with increasing pressure (Table 7).

It is a much more difficult problem to predict even the sign of γ_{ai} for ions in ice. It was believed initially that, owing to Coloumb attraction of the dipole moments of neighboring water molecules,

Table 6. Data on high-frequency (σ_∞) and static (σ_s) conductivities of ice.

Type of ice	T (°C)	σ_∞ $(\Omega m)^{-1}$	σ_s $(\Omega m)^{-1}$	$E_{S\infty}$ (eV)	$E_{\sigma s}$ (eV)
4 zone refinings	−10	—	4×10^{-9}	—	0.54
single crystals	—	—	2.5×10^{-8} (0...−20°C)	—	0 − 0.06
single crystals	−4 ... −56	—	6.4×10^{-10} (−10°C)	0.53 ± 0.01	0.70 ± 0.07
single crystals	−10	—	10^{-7}	0.37	—
single crystals	—	—	—	0.624	—
single crystals pure and HF-doped	−10	1.6×10^{-5}	1.1×10^{-7}	0.575	0.61
single crystals	0	—	2.5×10^{-8}	—	—
single crystals	−10	—	$(1.1 \pm 0.5) \times 10^{-8}$	0.76 ± 0.06	—
single crystals	—	—	2.3×10^{-8}	—	0.49
single crystals	−10	1.8×10^{-5}	—	0.61	—
single crystals	−10	—	—	—	—
HCl doping 10⁻⁵ mol/L	≥−39	—	—	0.492 ± 0.025	0
HCl doping	−39	—	—	0.259 ± 0.003	0.267 ± 0.009
KOH doping 0.1 mol/L (in solution)	0... −150	$2 \times 10^{-5} - 10^1$	up to 10^{-1}	0 ($T \leq -70°C$)	0.85 ($T < -70°C$)
KOH doping 0.032 mol/L (in solution)	−23... −203	$\sim 2 \times 10^{-4}$ (−23°C)	10^{-4} (−23°C)	0 ($T > -100°C$)	0.4 ($T > -100°C$)

16

ions will contract the lattice, i.e., $\gamma_{ai} < 0$. Experimental data shown in Table 7 refuted this opinion, and the activation volumes of both H_3O^+ and OH^- ions turned out to be positive. We can try to explain this by the fact that dipole moments of all neighboring molecules in the ice structure cannot be oriented towards the ion. This would result in a violation of the Bernal-Fowler rules. Also, if a dipole moment is directed away from the ion, it will be repelled rather than attracted, increasing the volume around the defect. Thus, such simple considerations are not sufficient to estimate γ_{ai} of ions, and ab initio calculations taking into account the permitted configurations of water molecule orientations in ice are required.

For a defect to jump from one molecule to the neighboring one (or from one bond to another one), an additional change in volume γ_{mi} may be required. This is rather obvious, since the energy of the transitional state of a defect is of course not lower than the energy of the equilibrium state. Therefore, when considering a defect transfer un-

der pressure, we have to add an additional term to the activation energy of their motion E_{mi}

$$E_{mi}(P) = E_{mi}(0) + \gamma_{mi} P. \qquad (61)$$

In other words, the amplitude of the potential relief shown in Figure 1 varies with pressure. During ion transfer, which, according to experimental data, occurs through a non-activational hop of protons along a bond, the crucial factor may be an exponential increase in the probability of such a transition attributable to a decrease in the length of the hydrogen bond owing to the applied pressure. This would appear as a negative activation volume γ_{mi}.

In the course of studies on the dependence of partial conductivities of defects σ_i on pressure, it was found that

$$\sigma_i = |e| \, \mu_i n_i \propto$$

$$\exp\left(\frac{[E_{ai}(0) + E_{mi}(0)] + P[\gamma_{ai} + \gamma_{mi}]}{k_B T}\right). \qquad (62)$$

Table 6 (cont'd).

E_{ai} (eV)	E_{aB} (eV)	Activation energy of ion mobility (eV)	Activation energy of D- and L-defect mobility (eV)	τ_D (s)	E_τ (eV)	Reference
1.08	—	—	—	—	—	Wörz and Cole (1969)
1.1	—	—	—	5.18×10^{-5} $(-10°C)$	0.598	Maidique et al. (1970)
1.4	—	—	—	—	—	Petrenko et al. (1983)
—	—	—	—	—	—	Bullemer and Riehl (1966)
—	—	—	—	5×10^{-5}	—	Camplin et al. (1978)
1.22	0.68	0	0.235	2×10^{-5} $(0°C)$	0.575	Jaccard (1959)
—	—	—	—	1.8×10^{-5}	0.59	von Hippel et al. (1971) Maidique et al. (1971)
—	—	—	—	—	—	Bullemer et al. (1969)
0.98	—	—	—			Maeno (1973)
—	—	—	—	4.5×10^{-5}	0.64	Camplin and Glen (1973)
—	—	—	—	10^{-4}	0.57	Zaretskii et al. (1989)
—	—	0	—	—	0.567 ± 0.00 90.293 ± 0.034	Takei and Maeno (1984)
—	0.79	0	0.19	—	—	Takei and Maeno (1987)
—	—	0	—	2×10^{-5}	0 $(T < -70°C)$	Zaretskii et al. (1988)
—	—	0	—	—	—	Howe and Whitworth (1989)

Table 7. Activation volumes of protonic point defects in ice. The data are given in the units of V_{mol} = 3.3×10^{-23} cm^3.

Ice type (concentrations in mole/L)	γ_{a1} (H$_3$O$^+$ ion)	γ_{a2} (OH ion)	γ_{a3} (D-defect)	γ_{a4} (L- defect)	$\gamma_{a1,2} + \gamma_{m1,2}$	$\gamma_{a3,4} + \gamma_{m3,4}$	Reference
pure polycrystals	—	—	—	—	$-(0.55 \pm 0.15)$	0.145 ± 0.015	Chen et al. (1965)
pure single crystals	—	—	—	—	$-(0.18 \pm 0.01)$	0.13 ± 0.01	Taubenberger et al. (1973)
$\approx 5 \times 10^{-6}$ HF	—	—	—	—	0.091 ± 0.024	$-(0.16 \pm 0.024)$	Taubenberger et al. (1973)
$\approx 3 \times 10^{-5}$ HF	—	—	—	—	0	$-(0.36 \pm 0.05)$	Taubenberger et al. (1973)
pure single crystals	—	—	—	—	$-(3 \pm 0.9)$	≈ 0.15 ($-25°$C)	Hubmann (1978)
10^{-4} NH$_3$	—	—	—	—	≈ -0.7	≈ 0.27 ($-25°$C)	Hubmann (1978)
3×10^{-4} HF	—	—	—	—	≈ -0.55	≈ 0.15 ($-25°$C)	Hubmann (1978)
single crystals 10^{-4} HCl	3.3 ± 0.12	—	—	1.33 ± 0.3	—	—	Evtushenko and Petrenko (1991)
single crystals 10^{-4} HF	3.9 ± 0.36	—	—	1.0 ± 0.39	—	—	Evtushenko and Petrenko (1991)
single crystals 10^{-4} NH$_3$	—	0.82 ± 0.39	0.7 ± 0.3	—	—	—	Evtushenko and Petrenko (1991)

We can determine only the "total" activation volume $[\gamma_{ai} + \gamma_{mi}]$. Such measurements were originally performed by Chen et al. (1965) on pure polycrystalline ice. They found that the static conductivity σ_s increases and the high-frequency conductivity σ_∞ decreases with increasing pressure. Similar measurements on monocrystalline ice were performed later by Taubenberger et al. (1973) and Hubmann (1978). Taubenberger et al. used pure and HF doped ice and Hubmann used pure and NH$_3$ and HF doped ice. The idea of using the doped ice was to produce a known initial concentration of various defects to separate out γ_{ai} and γ_{mi}. However, the interpretation of the results obtained from the doped ice still remains complicated and ambiguous, since pressure can affect the dissociation energies of protonic defects from impurities. Table 7 contains values of $(\gamma_{ai} + \gamma_{mi})$ found in these works. Here, we assume that σ_∞ and τ_D^{-1} are proportional to the partial conductivity of the majority charge carrier and that σ_s is proportional to the partial conductivity of the minority charge carrier, in conformity with eq 49–51. In the analysis of data presented in Table 7, we have to take into account that in the case of doped ice E_{ai} is related, obviously, to the energy of separation of a defect from an impurity.

Evtushenko and Petrenko (1991) used a quite different approach to determine activation volumes of protonic defects in ice. Since the formation energy of defects E_{ai} depends on the applied pressure P according to eq 57, in the presence of a pressure gradient there is a force $\vec{F}_i$ acting upon the defects

$$\vec{F}_i = -\text{grad}(E_{ai}) = -\gamma_{ai}\ \text{grad}(P). \qquad (63)$$

In their work, Evtushenko and Petrenko introduced a pressure gradient by bending thin ice samples and then measured the electric field strength $\vec{E}$ compensating for the effect of the force $\vec{F}_i$

$$e_i\ E = -\gamma_{ai} \text{grad}(P). \qquad (64)$$

By varying temperature and doping, they determined activation volumes of all four types of protonic defects in ice (see Table 7). The advantage of this method is that it enables us to separate out E_{ai} (i.e., the additional term to the specific volume of a defect) from the sum $E_{ai} + E_{mi}$. The results presented in the table are expressed in terms of the volume occupied by a water molecule in ice: 3.3×10^{-23} cm^3. According to the results of Evtushenko and Petrenko, all protonic defects (except H$_3$O$^+$

ion) have approximately doubled volume compared to the molecular volume.

Spectroscopic study of protonic defect migration—D–H exchange

An original and informative optical method of investigating protonic defects in ice was developed by Devlin (Ritzhaupt and Devlin 1977; Ritzhaupt et al. 1978, 1980; Devlin 1990). The method is based on the optical detection of hydrogen isotope exchange (H and D) between water molecules in ice. Since such an exchange can occur only through protonic defect transfer, the rate of isotope exchange enables us to estimate the diffusion of ions and Bjerrum defects in ice. Figure 8

illustrates the essence of this method. If we place a D_2O molecule in H_2O ice, then, because of the transfer of ions displacing protons and deuterons along hydrogen bonds, pairs of HOD molecules will be formed on adjacent sites. We shall denote these pairs as $(HOD)_2$. Hence, the rate of the reaction

$$D_2O + H_2O \rightarrow (HOD)_2 \qquad (65)$$
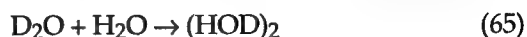
will be determined by the number of intermolecular jumps by ions, which is proportional to the ionic conductivity σ_{ion}.

For two deuterons to move a large distance apart, it is necessary to transfer a deuteron from one bond to another. This can take place only
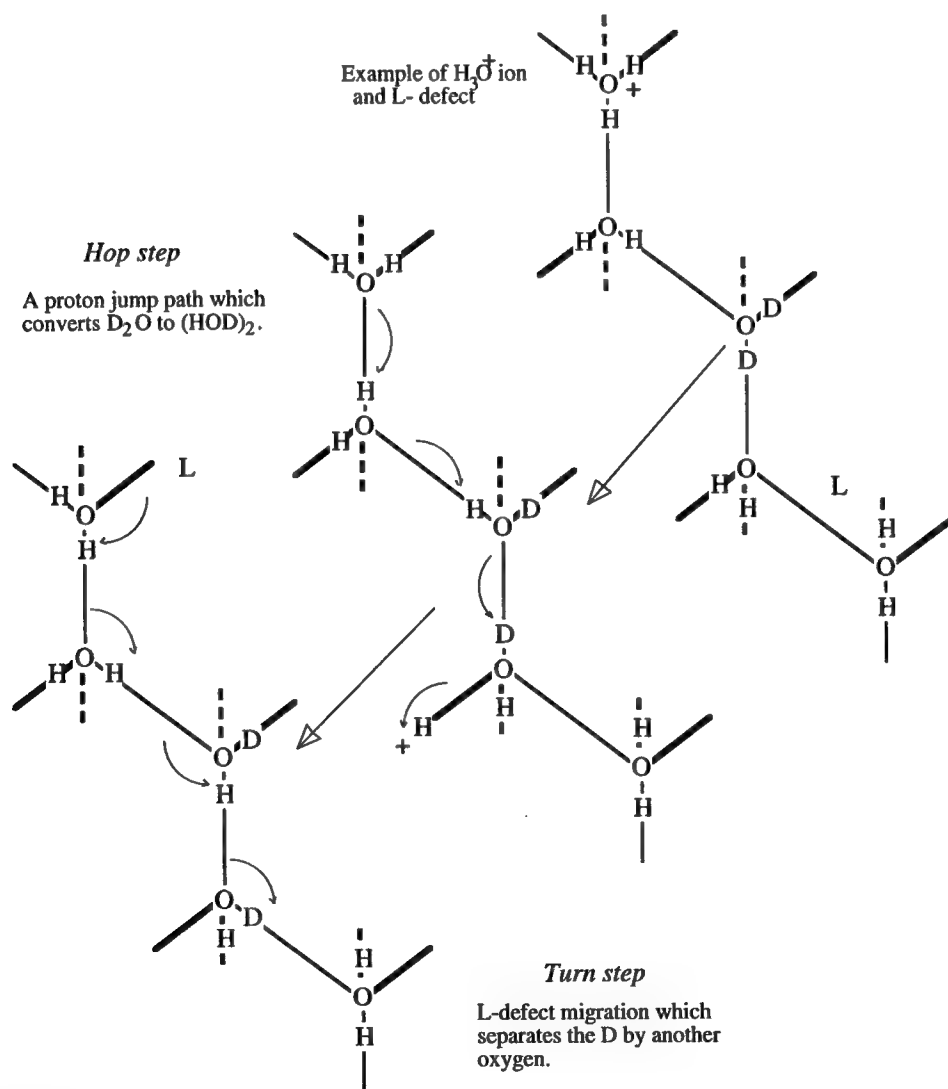
Figure 8. Point defects in an ice lattice, showing the proton hop step and the L-defect turn step of proton transport and isotopic exchange.

19

through Bjerrum defect migration. Therefore, the rate of the reaction

$$(HOD)_2 \rightarrow HOD + HOD \qquad (66)$$

will be determined by the number of elementary jumps of Bjerrum defects per second, which is proportional to $\mu_B\, n_B \propto \sigma_B$.

The reactions (eq 65–66) can be observed because the infrared absorption spectra of D_2O, $(HOD)_2$ and isolated HOD are different, as shown in Figure 9. Devlin and co-authors prepared H_2O ice samples with a small addition of D_2O by vapor deposition in a vacuum at 125 K. At such a low temperature, the protonic defect transfer is negligibly small and the ice obtained has the cubic structure I_c. Varying the temperature in 5-K steps and observing the kinetics of the changes in the IR spectra, Devlin and co-authors (Collier et al. 1984) found that in their samples in the temperature range from 130 to 150 K
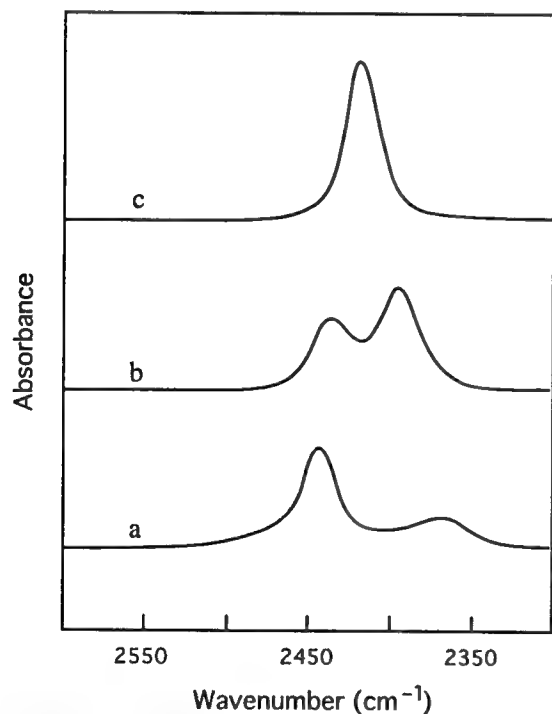
$$E_{\sigma i} \approx 0.41 \text{ eV}$$
and $\qquad\qquad\qquad\qquad\qquad\qquad (67)$
$$E_{\sigma B} \approx 0.52 \text{ eV}$$

which, although close to the values determined from electrical conductivity (see Table 6), are still considerably lower than the conventional values at higher temperatures. This discrepancy may be attributed to a number of factors, including extrinsic defect activity, the cubic nature of the ice used, or the predicted behavior ignoring shallow proton trapping,* or all three.

Probably the major significance of the work of Devlin and colleagues is that they confirmed at the

---

*The shallow proton traps were identified with the negatively charged L-defects (Kunst and Warman 1983). An association energy of a proton on such a trap was found as ≈ 0.43 eV by Woodbridge and Devlin (1988) and ≈ 0.19 eV by Kunst and Warman (1983).

Figure 9. Infrared spectra for isotopomers of H_2O decoupled in H_2O ice at 90 K: (a) D_2O; (b) $(HOD)_2$; (c) HOD (after Devlin 1992).

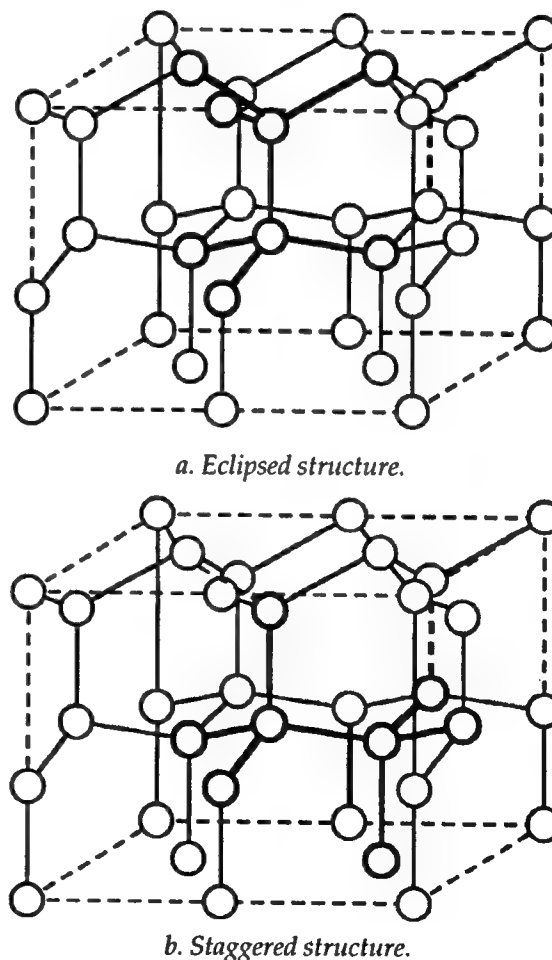a. Eclipsed structure.

b. Staggered structure.

Figure 10. Oxygen atom positions in ice I_h.

molecular level the two-step character of proton transfer in ice, and consequently the necessity for such a transfer to be performed by two groups of very different defects: ions and Bjerrum defects. In other words, the work of this group provides very strong support for the existence of both types of protonic defects in ice. Readers interested in this question can find details in the review by Devlin (1990). We shall also return to this topic in the report *Optical Properties of Ice*.

Atomic structure of protonic defects

The atomic structure of protonic defects depicted in Figure 4b is purely schematic. The introduction of a defect changes considerably the forces acting between adjacent atoms, and this leads to lattice "relaxation" around the defect. One piece of evidence for such relaxation is the increased specific volume of defects as compared to the molecular volume (see the *Activation Volume of Protonic Defects* section). The necessity for atomic rearrangement of the ice lattice around protonic defects can be demonstrated by estimation of the electrostatic energy of interaction between two protons on the same hydrogen bond in a D-defect. If we do not take relaxation and lattice rearrangement into account, then the two protons will be at a distance r of about 0.7 Å from each other. Since at such small distances we have to use $\varepsilon = 1$, the electrostatic energy of such a D-defect would be

$$\Delta E \approx \frac{e^2}{4\pi r \varepsilon_0} \approx 19 \text{ eV}. \tag{68}$$

This is extremely large compared to the observed formation energy of 0.68 eV of a pair of L- and D-defects.

Currently, there are two models in which the energy of protonic defects is lowered by rearrangement of atoms around a defect. In the first model, after a protonic defect is formed in the simplified fashion shown in Figure 4b, atoms and molecules are allowed to shift slightly from their initial positions. The new equilibrium stable configuration is the one with the lowest energy. This approach to the calculation of energy and structure of Bjerrum defects in ice was used by Plummer (1987, 1992). She used ab initio computer simulations, requiring very large amounts of computer time, and because of this only clusters comprising eight water molecules with a Bjerrum defect in the middle could be simulated. Two ways of choosing such clusters with "eclipsed" and "staggered" structure are shown in Figure 10. The new interatomic distances and energies ΔE for the formation

Table 8. Calculated parameters of Bjerrum defects (after Plummer 1992).

Parameter	Eclipsed	Staggered
D-defect		
O–O distance (Å)	3.30	2.72
H–H distance (Å)	1.78	2.23
Creation energy (eV)	0.417	0.278
L-defect		
O–O distance (Å)	3.18	3.16
Creation energy (eV)	0.317	0.343

of L- and D-defects in such clusters are summarized in Table 8.

Since in a real ice lattice Bjerrum defects can be located at hydrogen bonds both parallel (eclipsed structure) and inclined (staggered structure) to the hexagonal *c*-axis, we should take some average between the eclipsed and staggered values for comparison with experimental values, taking into account that there are three times more bonds inclined to the *c*-axis than are parallel to it. The results of this averaging are given in Table 9, along with values for the ideal ice structure I_h, but we must remember that the defects have been modeled not in bulk ice but in a cluster of only eight molecules.

The first thing that attracts our attention is that the length of the bond carrying the defect has increased. This increase is larger for L-defects, which is in qualitative agreement with the larger activation volume for L-defects found experimentally (Table 7). Plummer discovered a large increase in the H–H distance in a D-defect. One of the protons actually moves off the hydrogen bond, taking an interstitial position, and the remaining hydrogen bond becomes bent in the opposite direction by approximately 20°.

It is quite remarkable that, in spite of the small size of simulated clusters, the energy of pairs of L-

Table 9. Average parameters of Bjerrum defects in ice.

Parameter	Defect		Perfect structure
	D	L	
O–O distance (Å)	2.865	3.17	2.76
H–H distance (Å)	2.12	–	0.76
Creation energy (eV)	0.312	0.336	–

a. Ionic defect in one-dimensional chain of hydrogen bonds.

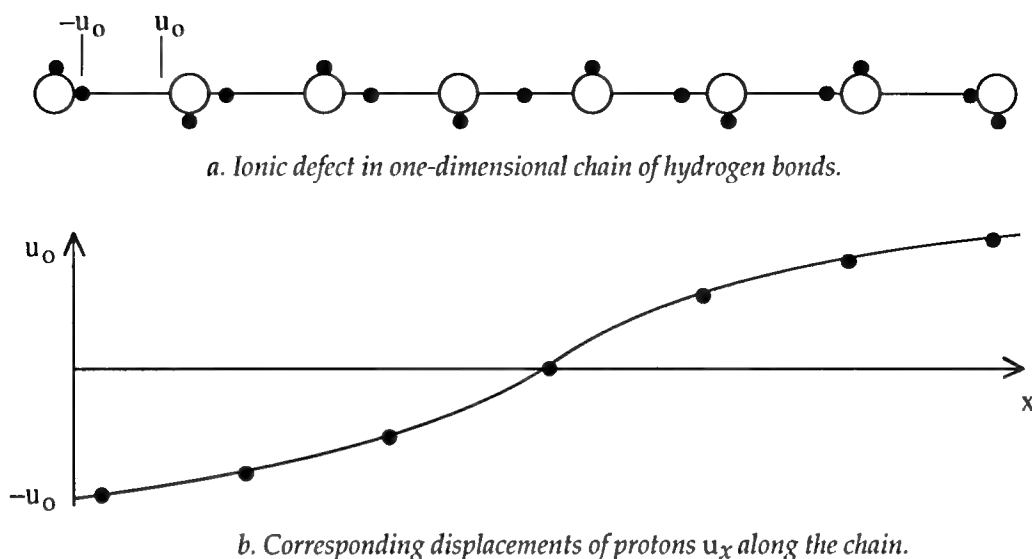*b. Corresponding displacements of protons* u_x *along the chain.*

Figure 11. Soliton model of OH$^-$ ion.

and D-defects according to Plummer is about 0.65 eV, which is very close to the value 0.68 eV found from experiments.

We can make one more interesting conclusion from Plummer's calculations by observing that energies of defects in "eclipsed" and "staggered" configurations are different. Because in diffusion and electrical conductivity processes, Bjerrum defects must flip from one configuration to an-

other, the difference in corresponding energies may contribute to the observed activation energy of defect migration. For L-defects this difference is only 0.026 eV (i.e., on the order of k_BT), whereas for D-defects it is equal to 0.14 eV. Is this not the reason for lower mobility of D-defects compared to L-defects? Calculations of the type performed by Plummer are quite complicated and have not yet been made for ions.
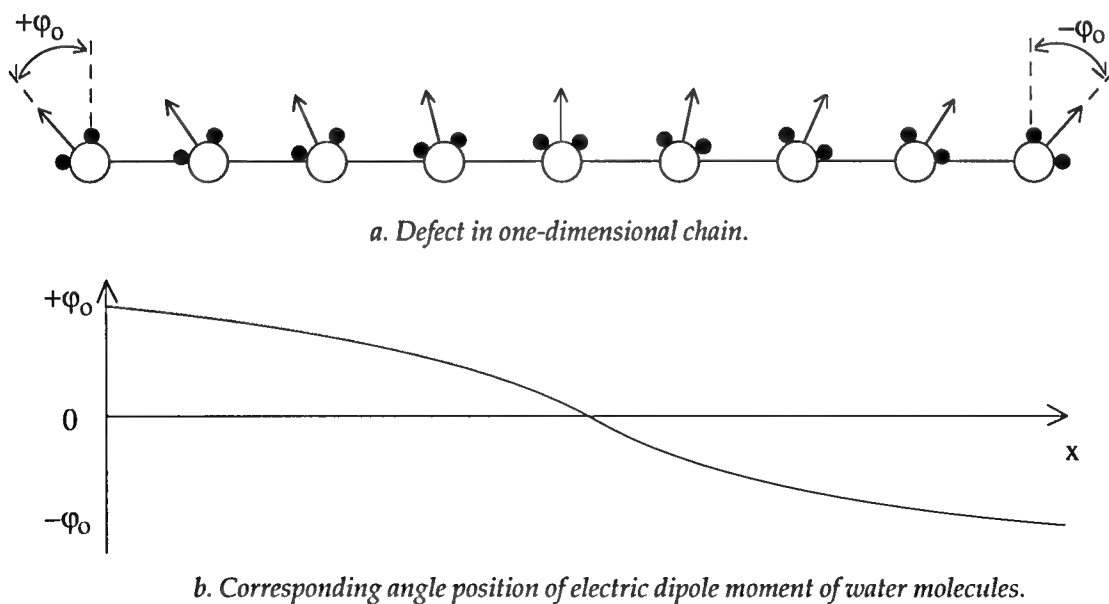

a. Defect in one-dimensional chain.

b. Corresponding angle position of electric dipole moment of water molecules.

Figure 12. Soliton model of Bjerrum defect.

22

The second type of model of the atomic structure of protonic defects is the so-called soliton model, in which the defect is spatially delocalized over several lattice sites. Both electrostatic and elastic energies of the defect are lowered by this. Originally suggested for the description of ion transfer along hydrogen bond chains by Antonchenko et al. (1983) and for Bjerrum defects by Sergienko (1986), this model has been further developed in many papers; it has numerous advocates and no less numerous opponents. A detailed theoretical description of this model can be found in a recent book by Davydov (1991). A simplified diagram of an OH⁻ "soliton ion" in a linear chain of hydrogen bonds is shown in Figure 11. Notice that all protons to the left of the center are displaced to the left end of their bonds and all protons on the right are displaced to the right. During the migration of such an ion to the right, the protons on the bonds are transferred to the left. For a soliton to arise and remain stable, at least two conditions must be satisfied: 1) the protons must behave cooperatively, i.e., they must strongly interact with each other, and 2) a strong nonlinear interaction of the proton and oxygen sub-lattices is required.

The soliton simulating an L-defect (the migration of the defect from left to right transfers the protons from right-side positions on the bonds to left-side positions) is shown in Figure 12. Using the same schematic, the reader can easily construct an H_3O^+ ion and a D-defect. Since the transfer of soliton defects results in exactly the same changes in the positions of protons on the bonds as in the case of transfer of their "point" analogs, the formal description of their effects in the ice, effective charges, contributions to $\vec{\Omega}$, etc., will be exactly the same.

In spite of a certain elegance of the soliton model, serious arguments have appeared against its applicability to ice. The first argument presented by Nagle (1992) is that solitons, requiring for their motion a coordinated displacement of protons arranged into some ordered positions, will just get "stuck" in a disordered ice protonic structure. A second objection is that the soliton is defined and has to move along a particular track, whereas the bonds in ice form a branched network. The relaxed state of a static defect may in reality be somewhat delocalized, but the theory of solitons is essentially dynamic.

A third objection to the soliton model in ordered water molecule chains arises from precise ab initio calculations performed by Godzik (1990) and Scheiner (1991). These calculations show that in ordered chains of H_2O molecules the cooperative motion of several protons involves a significantly higher energy barrier than that for successive jumps of one proton after another.

We cannot leave the structure of protonic defects without mentioning the possibility that these defects could be coupled with vacancies (Kröger 1974). For example a D-defect at a vacancy is merely a vacant site with three rather than the normal two hydrogen bonds pointing into it, and its D character will move with it as it moves through the lattice (see Fig. 17). As vacancies may be highly mobile, we must allow for the possibility that the majority of Bjerrum defects could exist and move in this way. There is, however, no experimental evidence on this issue.

IMPURITIES

Although liquid water is a very good solvent for many substances, its solid phase—ice—dissolves almost nothing. Most of the impurities dissolved in water either get rejected as the water freezes or precipitate as a second phase within the ice. There are some exceptions, such as a few acids (HF, HCl), ammonia (NH_3), some alkalis (KOH, NaOH) and their derivatives like NH_4F. These substances can be incorporated properly into the ice structure where they drastically change the protonic carrier concentrations in the ice. To understand how these impurities affect the electrical properties of ice, let us consider the probable patterns of their incorporation into the ice lattice (see Fig. 13–15). Note that although there now exist a number of experimental techniques for investigating crystal structures on an atomic scale (high resolution transmission electron microscopy, scanning tunneling microscopy, atomic force microscopy, etc.), such techniques have not yet been successfully applied to ice. Patterns such as those represented in Figures 13–15 turn out to be just hypotheses based upon ionic radii, energies and lengths of atomic bonds, etc. The ionic radius of F^-, for example, is rather close to that of O^{2-}, and it is natural to assume that fluorine substitutes for oxygen successfully in an ice lattice. As can be seen from Figure 13, since the HF molecule can provide only one proton for the four nearest hydrogen bonds, one bond appears to be lacking any protons at all; i.e., substitution of the water molecule by the HF molecule results in the appearance of an L-defect associated with the impurity molecule. The binding energy of such an L-defect with the HF molecule is not large ($\leq 10^{-2}$

eV [Jaccard 1959, Camplin et al. 1978]). Since the number of possible arrangements of the L-defect in an ice lattice is enormous, practically all L-defects leave their parent molecules.

Moreover, it turns out that the single proton in the HF molecule is not bound firmly and can jump along a hydrogen bond to another water molecule, turning that water molecule into an H_3O^+ ion. It is important to emphasize the chemistry of HF. To a physicist the natural thing would be for an extra proton to attach to HF, forming an OH^- ion, but chemically HF is a weak acid in water and prefers to lose a proton.

At the same time as HF doping of ice increases the L-defect and H_3O^+ ion concentrations, it will also lower the concentrations of D-defects and OH^- ions. This happens because the equilibrium concentrations of D-defects and OH^- ions in pure ice are determined by a balance between the rate of their thermoactivated production and the rate of
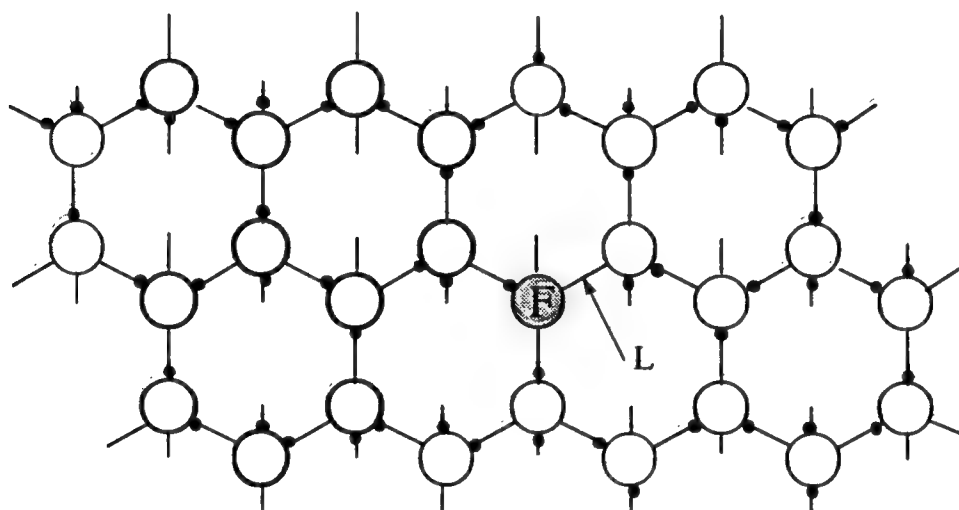
a. Ice lattice with incorporated HF molecule.
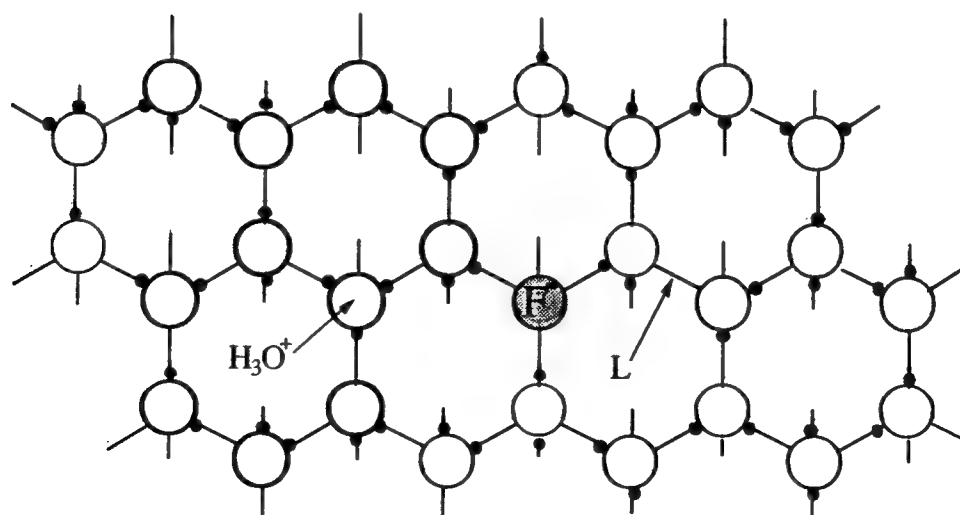
b. Same after H_3O^+ ion and L-defect were released by means of sequential hops of protons (along the hydrogen bonds to release H_3O^+ ion and between the bonds to release L-defect).
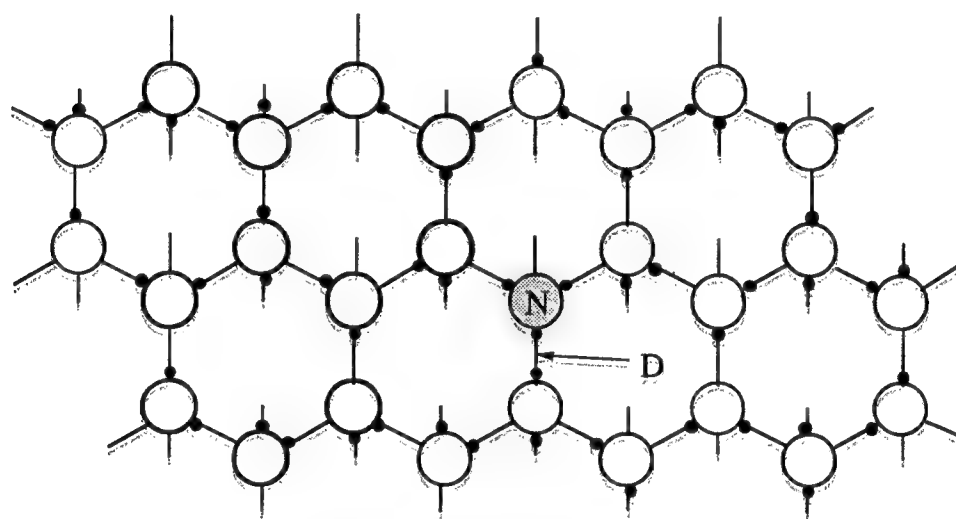
Figure 13. Hypothesized pattern of incorporation of HF impurity.

recombination: D- with L-defects and H_3O^+ with OH^- ions. HF doping increases L-defect and H_3O^+ ion concentrations, so that the rate of recombination increases, which results in decreasing D-defect and OH^- ion concentrations. This can be stated in terms of the law of mass action, which is that the products of concentrations $n_1 \times n_2$ and $n_3 \times n_4$ must be constant in thermal equilibrium, irrespective of doping

$$n_1 \times n_2 \approx \frac{4}{9}\left(n_{H_2O}\right)^2 \exp\left(-\frac{E_{ai}}{k_B T}\right), \quad n_{1,2} \ll n_{H_2O} \quad (69)$$

$$n_3 \times n_4 \approx \left(n_{H_2O}\right)^2 \exp\left(-\frac{E_{aB}}{k_B T}\right), \quad n_{3,4} \ll n_{H_2O}. \quad (70)$$

Another molecule that can successfully be incorporated into the ice lattice, substituting for water molecules, is ammonia, NH_3 (Fig. 14). Since NH_3 donates three protons (instead of two as in the case of H_2O) for four hydrogen bonds, we observe two protons at one bond at the same time, i.e., a D-defect. As a consequence of the thermoactivation process, this defect can be released and take part in the conductivity process.

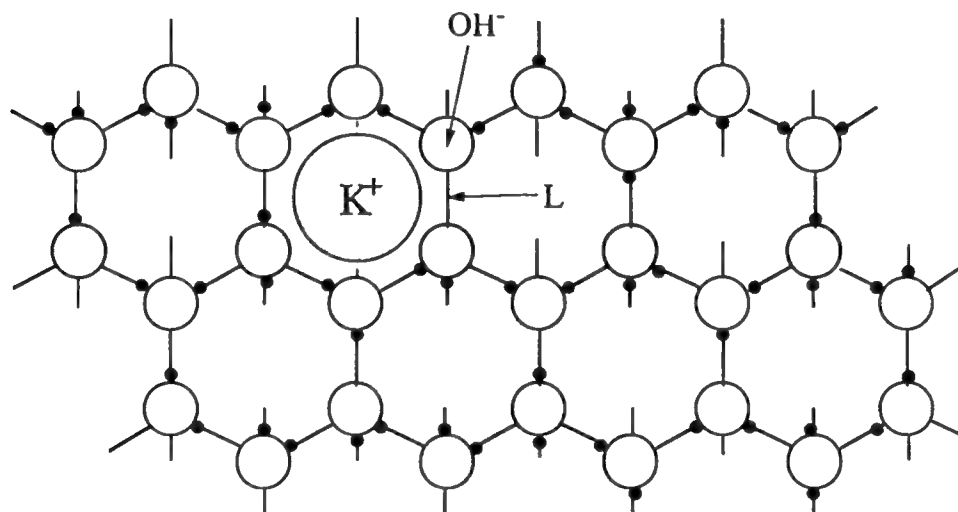a. NH_3 molecule incorporated into ice structure.
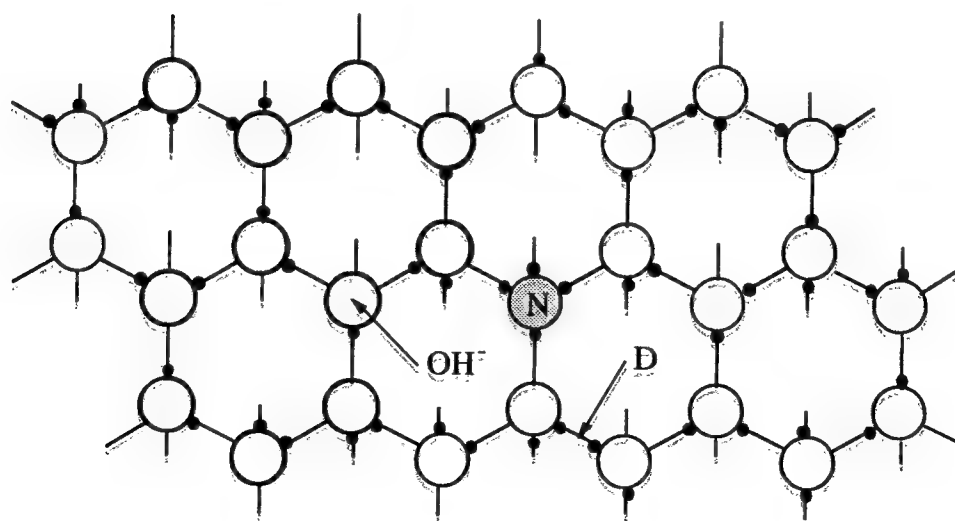
b. Same after release of OH^- ions and D-defect from the NH_3 molecule.

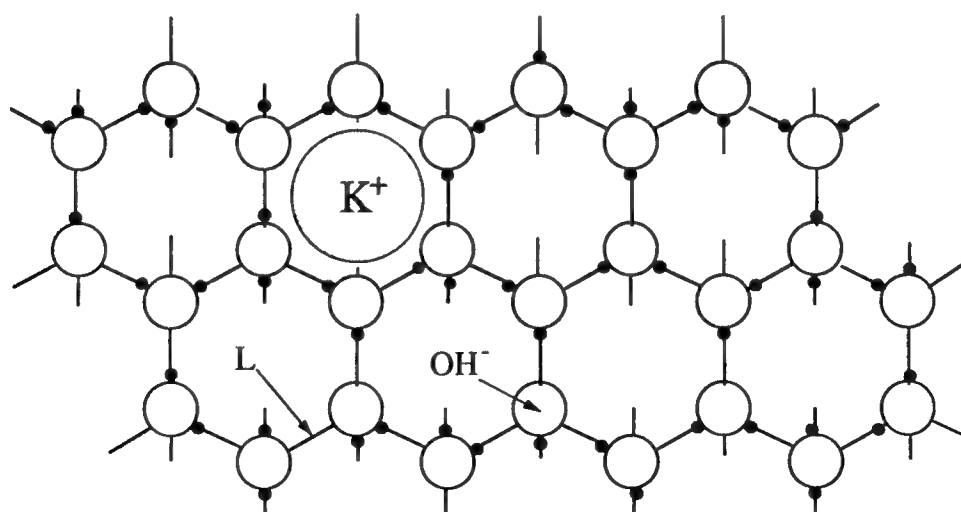Figure 14. Hypothesized pattern of incorporation of NH_3 impurity.

Besides, the NH_3 molecule is a base and can accept a fourth proton, forming an OH^- ion at a neighboring water molecule. Activation energies for the release of D-defects and OH^- ions from the ammonia molecule in ice are comparatively large, so that, although ammonia doping of ice increases D-defect and OH^- ion concentrations (decreasing L-defect and H_3O^+ ion concentrations in accordance with eq 69–70), its influence in terms of conductivity is not as efficient as that of HF. It is also important that NH_3 doping increases the concentration of less mobile carriers (D-defects and OH^- ions); see Table 6.

Lastly, the third, very important group of impurities that considerably affect the conductivity of ice are the alkali hydroxides, among which the most significant is KOH. The most plausible mechanism of incorporation of KOH into the ice struc-

a. How KOH dissolved in ice is thought to introduce defects. The K^+ ion is interstitial, the OH^- ion substitutes for a water molecule leaving one bond without any proton—an L-defect.

b. Same after L-defect and OH^- ion have moved away from the K^+ ion.

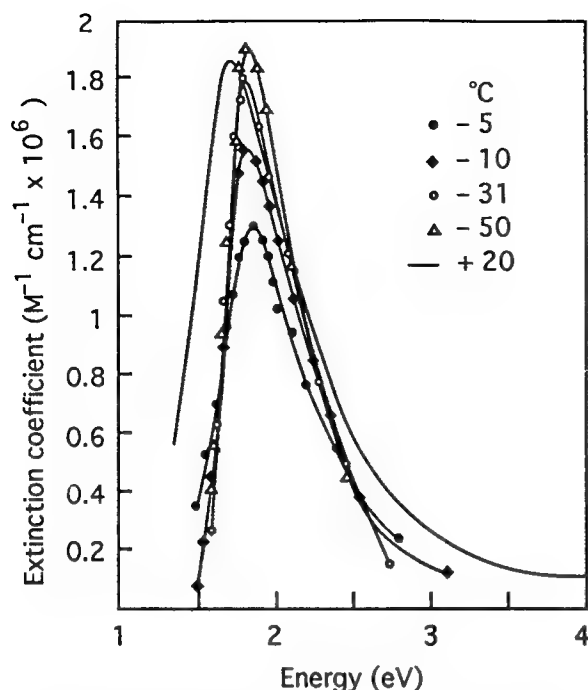Figure 15. Hypothesized pattern of incorporation of KOH impurity.

Figure 16. Absorption spectra of solvated electrons in water and ice (after Nilsson et al. 1972).

ture is shown in Figure 15. The potassium atom is accommodated in interstices, while the hydroxyl group OH is built into the lattice. As can be seen from Figure 15, this results in the appearance of L-defects and OH⁻ ions linked to KOH impurity. Thermoactivation processes allow them to be released into the ice bulk, increasing L-defect and OH⁻ ion concentrations and suppressing D-defects and H_3O^+ ions. Because of the extremely small binding energies of L-defects and OH⁻ ions with K^+ ions in ice, these impurities become efficient donors of L-defects and OH⁻ ions even at very low temperatures (Zaretskii et al. 1988).

The subject of the concentrations of charge carriers in doped ice has been treated many times in the scientific literature (see Jaccard 1959, Kröger 1974, Camplin et al. 1978), and is described more fully in the report on the *Electrical Properties of Ice* (Petrenko 1993a). For the fullest detail, based on the law of mass action, the reader is referred to Kröger (1974).

At present there are hundreds of papers available in the literature in which the electrical properties of doped ice were studied. The results of these studies were discussed in detail in the review by Petrenko (1993a) and are presented in part in Tables 4–6. Let us refer to the following works as

examples: Takei and Maeno (1984, 1987) on HCl doped ice; Gross (1975) and Gross et al. (1978) on HCl, HF, NaCl, KF, NH_4F, NH_4OH, NH_4Cl, NH_4HCO_3 doped ice; KOH doped ice was studied by Zaretskii et al. (1988) and by Howe and Whitworth (1989).

On the whole, the effect of impurities dissolved in ice on its electrical properties is rather well explained on the basis of the currently accepted model of electrical conductivity of ice, provided that the concentrations of all four types of charge carriers are calculated following the method suggested by Kröger (1974).

The impurity diffusion coefficients in ice were measured in a number of works. Haltenorth and Klinger (1969, 1977) investigated diffusion of HF in monocrystalline ice parallel and perpendicular to the c-axis. They found that at $T = -10°C$ the diffusion coefficient of HF in ice is 1.08×10^{-11} m² s⁻¹ and obeys the Arrhenius law with an activation energy of 0.2 eV. The value of the diffusion coefficient along the c-axis was 20% lower than the corresponding value normal to it. In polycrystalline ice the diffusion coefficient was 25% higher than in monocrystals owing to grain boundary diffusion. It should be noted that the diffusion coefficient for HF is much larger than the self-diffusion coefficients of H_2O given in Table 2, which suggests that HF molecules move through interstitial positions more easily than those of H_2O.

Diffusion of the neutral gases He and Ne was studied by Haas et al. (1973). Diffusion coefficients of these gases in ice appeared to be extremely high, indicating a "transparency" of ice for these gases. It is interesting that the diffusion coefficients along the c-axis ($D_{||c}$) were six times (He) and eight times (Ne) higher than in the perpendicular direction. In the temperature range 173–253 K for He and 213–263 K for Ne, Haas and co-authors found that the following relationships hold

$$D_{||c}(\text{He}) = 3.4 \times 10^{-7} \exp\left(-\frac{0.12 \text{ eV}}{k_B T}\right) \text{ m}^2 \text{ s}^{-1} \quad (71)$$

$$D_{\perp c}(\text{He}) = 1.1 \times 10^{-7} \exp\left(-\frac{0.13 \text{ eV}}{k_B T}\right) \text{ m}^2 \text{ s}^{-1} \quad (72)$$

$$D_{||c}(\text{Ne}) = 1.2 \times 10^{-6} \exp\left(-\frac{0.25 \text{ eV}}{k_B T}\right) \text{ m}^2 \text{ s}^{-1} \quad (73)$$

ELECTRONIC DEFECTS

In this section we will consider point defects that arise from an excitation of the electronic subsystem of ice: hydrated electrons, radicals and
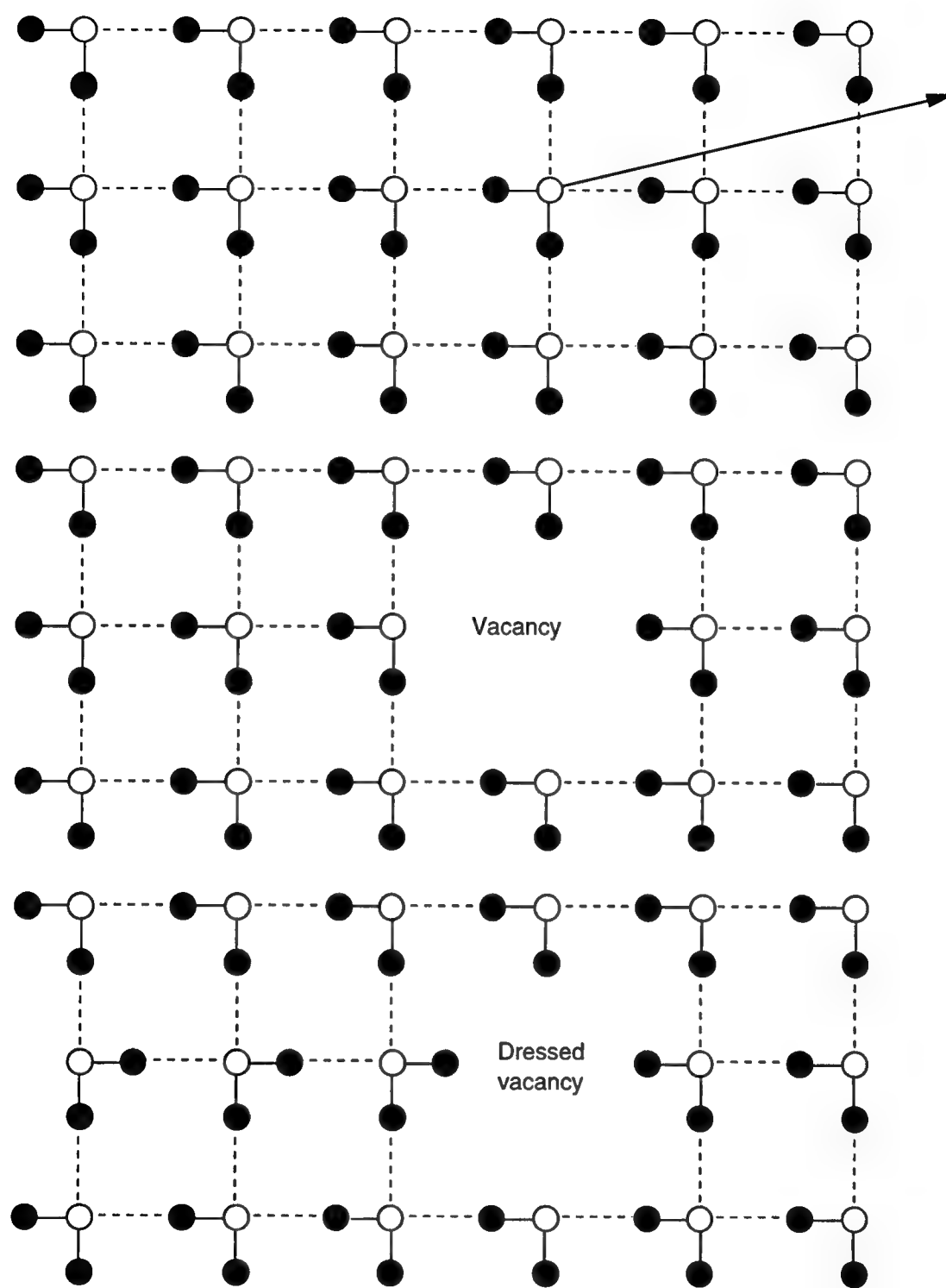
Figure 17. Complex (vacancy + D-defect) formation in ice (after de Haas et al. 1983).

color centers. Since ice has a very wide forbidden band with $E_G \approx 8.5$ eV (Ryzhkin 1992), the above excitations usually arise when ice is either illuminated by hard ultraviolet radiation or is excited by beams of charged particles, γ-rays and X-rays.

Conducting electrons in ice have been studied in many works (e.g., Verberne et al. 1978; Warman et al. 1980, 1982, 1983; de Haas et al. 1983; Kunst et al. 1983). Conducting electrons in these studies were excited either by a short X-ray pulse of about 0.5 ns, produced by irradiation of a Pt target with 3-MeV electrons from a Van de Graaf accelerator, or directly by the 3-MeV electron beam. The lifetime of electrons in the conduction band is extremely small; at $T = -20°C$ it is several nanoseconds and at $T = -60°C$ several tens of nanoseconds (de Haas et al. 1983). The main processes limiting the lifetime of electrons at these temperatures are trapping and solvation (hydration). In spite of small lifetimes, the analysis of transient electron currents in strong electric fields showed their mobility to be $\mu_e = (25 \pm 5) \times 10^{-4} m^2 V^{-1} s^{-1}$ (Verberne et al. 1978, Warman et al. 1980, 1982). This value, as the reader must have noticed before, exceeds the mobility of most mobile protonic charge carriers in ice by more than four orders of magnitude (see Table 5). The mobility of electrons in ice is almost independent of temperature from -60 down to $-120°C$.

All conducting electrons move very rapidly into the so-called solvated state. In the literature these electrons are often referred to as "solvated" or "hydrated" electrons; these terms are equivalent. Such electrons manifest themselves through a specific absorption spectrum with a maximum at approximately 6800 Å and through a distinct Electron Spin Resonance (ESR) line. Initially, solvated electrons were discovered in water and later in ice. A great number of publications are dedicated to solvated electrons and yet many of their properties remain unclear. Below, we shall address questions about the structure, lifetime, optical properties, recombination and mobility of solvated electrons in ice.

The major reason for electrons first to become localized and then to move into the solvated state is considered to be the polarization of the surrounding medium by the electron. Owing to a large dipole moment, water molecules tend to orient towards the electron. The electrostatic energy of the state in which the electron is "coated" by water molecules oriented towards it would be obviously less than the initial nonpolarized state. In water, where each molecule can be reoriented

extremely fast, such polarization would seem to occur in a different fashion than in ice in which the mutual molecular orientation follows the ice rules. Nevertheless, the optical absorption spectrum of the final, fully relaxed state of the trapped electron in ice resembles very closely that of the solvated electron in water, with only a small shift in the position of the absorption maximum at 1.8 eV being found upon melting (Nilsson et al. 1972, Shubin et al. 1966, Taub and Eiben 1968).

Several of such spectra in ice and one in water are shown in Figure 16. The observation of similar absorption spectra in water-containing media can be considered as evidence for the presence of solvated electrons. This similarity of the absorption spectra of solvated electrons in water and ice strongly suggests the same basic microscopic structure for the solvated state in both media. Present opinion, based on theoretical considerations and ESR studies of electrons in low-temperature aqueous glasses (Kevan 1981), tends to favor a cavity model for the solvated electron, i.e., a model in which the electron occupies a void surrounded by oriented water molecules. This being the case, the initial localization process in ice must therefore involve trapping at a vacancy in the lattice.

Figure 17, adopted from the paper by de Haas et al. (1983), shows schematically one of the possible structures of the solvated electron in ice. Such a defect is a combination of a water molecule vacancy, a D-defect and an electron (not shown). In this type of a defect, the electrostatic energy is lowered by attraction between the electron and three protons. A migration of this defect must be accompanied by cooperative drift of the vacancy and the D-defect. Their mobilities could have provided some estimation of the solvated electron's mobility in ice. Unfortunately, we could not find in the literature any reliable data on diffusion coefficients of either vacancies or D-defects or solvated electrons in ice. The mobility of solvated electrons in water was measured to be $1.84 \times 10^{-7} m^2 V^{-1} s^{-1}$ (Schmidt and Buck 1966). This value can be considered as an upper limit for mobility of solvated electrons in ice.
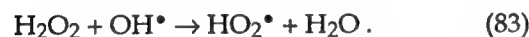
Both in water and ice, solvated electrons are annihilated by the recombination reaction (Muto et al. 1992)

$$e^- + H_3O^+ \rightarrow H_2O + H^\bullet \cdot \qquad (74)$$

In addition, they can react with impurities in the bulk and at the surface. All these factors reduce their lifetimes, which nonetheless can be very large

29

at low temperatures (about 80 minutes at 4.2 K [Muto et al. 1992]).

In eq 74 we have used the symbol "•" to denote a "radical," i.e., an atom or a molecule that has an unpaired electron spin. Owing to the presence of such an electron, the radicals are extremely chemically active and consequently unstable. In eq 74 we have a hydrogen radical or simply a hydrogen atom $H^\bullet$; $H^\bullet$ is not the only radical produced during ionization of water molecules in ice. We list below some most frequently encountered reactions in which radicals consisting of hydrogen and oxygen atoms are created and annihilated:

$$H_2O + h\nu \rightarrow H_2O^+ + e^- \tag{75}$$

$$H_2O^+ + H_2O \rightarrow H_3O^+ + OH^\bullet \tag{76}$$

$$H_3O^+ + e^- \rightarrow H_2O + H^\bullet \tag{77}$$

$$OH^\bullet + OH^\bullet \rightarrow H_2O_2 \tag{78}$$

$$H^\bullet + H^\bullet \rightarrow H_2 \tag{79}$$

$$H^\bullet + OH^\bullet \rightarrow H_2O \tag{80}$$

$$OH^\bullet + H_2O \text{ s} \leftrightarrows H_3O^+ + O^- \tag{81}$$

$$H_2O_2 + H^\bullet \rightarrow H_2O + OH^\bullet \tag{82}$$

$$H_2O_2 + OH^\bullet \rightarrow HO_2^\bullet + H_2O. \tag{83}$$
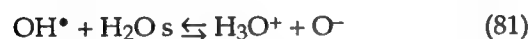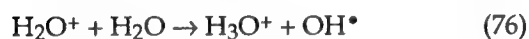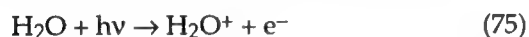
The study of the properties of radicals belongs to the extensive domain of radiation chemistry and falls outside the scope of this report. The reader interested in the properties of radicals in ice can find a detailed list of references on this question in the papers by Bednarek and Plonka (1987a,b) and also in the already cited references concerning free (conduction) and solvated electrons.

Let us indicate here that, because of the fractional charge of ions in ice ($\pm$ 0.62e), some of the reactions (eq 75–83) (written for water, where ions have an integer charge) must be altered and completed to fulfill the charge conservation law. For example, the charge of particles in the left-hand side of eq 77 is –0.38e, and that of the right-hand side is zero. The charge conservation law will hold if we add to the left-hand side a D-defect. In this case the electron is a solvated electron trapped by the complex: a water molecule vacancy + D-defect. Thus, now the reaction (eq 74) can be written as

$$H_3O^+ + (e^- + V_{H_2O} + D) \rightarrow H_2O + H^\bullet + V_{H_2O}. \tag{84}$$
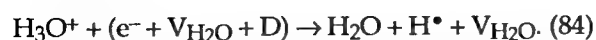
For the charge to be conserved in the above reaction (eq 77), we have either to add a D-defect to the right-hand side or to assume that the radical $OH^\bullet$ has a charge of +0.38e. The possibility for the radicals in ice to be electrically charged was first suggested by Chesnakov et al. (1987). The reasons for the radicals embedded in the ice structure to have an electric charge are the same that lead to the fractional charges of ions in ice. There is no experimental evidence available that supports or refutes the presence of electrical charge at radicals in ice.

LITERATURE CITED

Antonchenko, V. Ya., A.S. Davydov and A.S. Zolotariuk (1983) Solitons and proton motion in ice-like structures. *Physica Status Solidi (b)*, **115**: 631–640.

Bednarek, J. and A. Plonka (1987a) Single-crystal electron spin resonance studies on radiation-produced species in ice I_h. Part 1. The O^- radicals. *Journal of the Chemical Society, Faraday Transactions, 1*, **83**(12): 3725–3735.

Bednarek, J. and A. Plonka (1987b) Single-crystal electron spin resonance studies on radiation-produced species in ice I_h. Part 2. The HO_2 radicals. *Journal of the Chemical Society, Faraday Transactions, 1*, **83**(12): 3737–3747.

Ben–Naim, A. and F.H. Stillinger (1972) *Structure and Transport Processes in Water and Aqueous Solutions* (R.A. Horne, Ed.). New York: Wiley–Interscience.

Bullemer, B. and N. Riehl (1966) Bulk and surface conductivity of ice. *Solid State Communications*, **4**: 447–448.

Bullemer, B., H. Engelhardt and N. Riehl (1969) Protonic conduction of ice. In *Physics of Ice* (N. Riehl, B. Bullemer and H. Engelhardt, Ed.). New York: Plenum Press, p. 416–442.

Camplin, G.C. and J.W. Glen (1973) The dielectric properties of HF–doped single crystals of ice. In *Physics and Chemistry of Ice* (E. Whalley, S.J. Jones and L.W. Gold, Ed.). Ottawa: Royal Society of Canada, p. 256–261.

Camplin, G.C., J.W. Glen and J.G. Paren (1978) Theoretical models for interpreting the dielectric behavior of HF–doped ice. *Journal of Glaciology*, **21**(85): 123–141.

Chen, M.S., L. Onsager, J.C. Bonner and J.F. Nagle (1974) Hopping of ions in ice. *Journal of Chemical Physics*, **60**: 405–418.

Chen, R.K., D.W. Davidson and E. Whalley (1965) Effect of pressure on the dielectric properties of ice I. *Journal of Chemical Physics*, **43**: 2376–2383.

Chesnakov, V.A., V.F. Petrenko, I.A. Ryzkhin and A.V. Zaretskii (1987) Photoelectrical phenomena at ice–semiconductor interfaces. *Journal de Physique, C1*, **48**: 99–103.

Collier, W.B., G. Ritzhaupt and J.P. Devlin (1984) Spectroscopically evaluated rates and energies for proton transfer and Bjerrum defect migration in cubic ice. *Journal of Physical Chemistry*, **88**: 363–368.

Cotteril, R.M.J., J.W. Martin, O.V. Neilsen and O.B. Pedersen (1973) Computer studies of perfect crystal properties and defect structures in ice I. In *Physics and Chemistry of Ice* (E. Whalley, S.J. Jones and L.W. Gold, Ed.). Ottawa: Royal Society of Canada, p. 23–27.

Davydov, A.S. (1991) *Solitons in Molecular Systems*. Chapter 12. Dordrecht–Boston–London: Kluwer Academic Publishers.

de Haas, M.P., M. Kuust, J.M. Warman and J.B. Verberne (1983) Nanosecond time–resolved conductivity studies of pulse-ionized ice. 1. The mobility of conduction band electrons in H_2O and D_2O ice. *Journal of Physical Chemistry*, **87**: 4089–4092.

Devlin, J.P. (1990) Vibrational spectra and point defect activity of icy solids and gas phase clusters. *International Review of Physical Chemistry*, **9**(1): 29–65.

Devlin, J.P. (1992) Defect activity in icy solids from isotope exchange rates: Implications for conductance and phase transitions. In *Proton Transfer in Hydrogen-bonded Systems* (T. Bontis, Ed.). New York: Plenum Press.

Eckener, U., D. Helmreich and H. Engelhardt (1973) Transit time measurements of protons in ice. In *Physics and Chemistry of Ice* (E. Whalley, S.J. Jones and L.W. Gold, Ed.). Ottawa: Royal Society of Canada, p. 242–245.

Eigen, M. and L. De Mayer (1956) Ein stationäres Feldverfahren zur Untersuchung von Dissoziationsprozessen in Feüssigkeiten und Festkörpern. *Z. Elektrochem.*, **60**: 1037–1048.

Eigen, M. and L. De Mayer (1957) Berichtigungzu der Mitteilung. *Z. Elektrochem.*, **61**: 856.

Eigen, M. and L. De Mayer (1958) Self–dissociation and protonic charge transport in water and ice. *Proceedings of the Royal Society*, **A247**: 505–533.

Eigen, M., L. De Mayer and H. Spatz (1964) Über das Kinetische Verhalten von Protonen and Deuteronen in Eiskristallen. *Z. Elektrochem.*, **68**: 19–29.

Eldrup, M. and O.E. Mogensen (1978) Vacancies in HF-doped and irradiated ice by positron annihilation techniques. *Journal of Glaciology*, **21**(85): 101–112.

Evtushenko, A.A. and V.F. Petrenko (1991) Investigations of the pseudopiezoelectric effect and the stress–potential constants of charge carriers in ice. *Soviet Physics—Solid State*, **33**(5): 850–855.

Fletcher, N.H. (1970) *The Chemical Physics of Ice.* Cambridge University Press.

Glen, J.W. (1974) Physics of ice. USA Cold Regions Research and Engineering Laboratory, Monograph II-C2a.

Glen, J.W. (1975) Mechanics of ice. USA Cold Regions Research and Engineering Laboratory, Monograph II-C2b.

Godzik, A. (1990) An estimation of energy parameters for the soliton movement in hydrogen-bonded chains. *Chemical Physics Letters*, **171**(3): 217–221.

Gross, G.W. (1975) Dielectric relaxation spectrum and conductivity of ice crystals doped with ionic impurities. *Annual Report. Conference on Electric Insulation and Dielectric Phenomena*. Washington, DC: National Academy of Sciences, p. 347–358.

Gross, G.W., I.C. Hayslip and R.N. Hoy (1978) Electrical conductivity and relaxation in ice crystals with known impurity content. *Journal of Glaciology*, **21**(85): 143–160.

Haas, J.A., B. Bullemer and A. Kahane (1973) Diffusion and solubility of He and Ne in ice single crystals. *International Symposium on Physics and Chemistry of Ice, Ottawa*. (This paper was not published but its results are available in Hobbs [1974], p. 742).

Haltenorth, H. and J. Klinger (1969) *Diffusion of Hydrogen Fluoride in Ice* (N. Riehl, B. Bullemer and and H. Engelhardt, Ed.). New York: Plenum Press, p. 579–584.

Haltenorth, H. and J. Klinger (1977) Solubility of hydrofluoric acid in ice I_h single crystals. *Solid State Communications*, **21**: 533–535.

Hobbs, P.V. (1974) *Ice Physics.* Oxford: Clarendon Press.

Hondoh, T. (1992) Glide and climb processes of dislocations in ice. *Physics and Chemistry of Ice* (N. Maeno and T. Hondoh, Ed.). Sapporo: Hokkaido University Press, p. 481–487.

Hondoh, T., K. Azuma and A. Higashi (1987) Self-interstitials in ice. *Journal de Physique, C1*, **48**(3): 183–187.

Howe, R. and R.W. Whitworth (1989) The electrical conductivity of KOH–doped ice from 70 to 250 K. *Journal of the Physics and Chemistry of Solids*, **50**(9): 963–965.

Hubmann, M. (1978) Effect of pressure on the dielectric properties of ice I_h single crystals doped with NH_3 and HF. *Journal of Glaciology*, **21**(85): 161–172.

Hubmann, M. (1979a) Polarization processes in the ice lattice. Part I. *Z. Physik*, **32**: 127–139.

Hubmann, M. (1979b) Polarization processes in

the ice lattice. Part II. Z. *Physik,* **32**: 141–146.

Itagaki, K. (1967) Self-diffusion in single crystal ice. *Journal of the Physical Society of Japan,* **22**: 427–431.

Jaccard, C. (1959) Etude theorique et experimentale des proprieties electriques de la glace. *Helvetica Physica Acta,* **32**: 89–128.

Jaccard, C. (1964) Thermodynamics of irreversible processes applied to ice. *Physik der Kondensierten Materie,* **3**: 99–118.

Kevan (1981) Electron spin echo studies of solvation structure. *Journal of Physical Chemistry,* **85**: 1628–1636.

Kröger, F.A. (1974) Ice. In *The Chemistry of Imperfect Crystals,* 2nd ed. Amsterdam: North–Holland Publishing Co., p. 783–799.

Kuhn, W. and Thürkauf (1958) Isotopentrennung beim Gefrieren von Wasser und Diffusionkonstanten von D und ^{18}O im Eis. *Helvetica Chimica Acta,* **XLI**, IV(110): 938–971.

Kunst, M. and J.M. Warman (1983) Nanosecond time-resolved conductivity studies of pulse-ionized Ice. 2. The mobility and trapping of protons. *Journal of Physical Chemistry,* **87**: 4093–4095.

Kunst, M., J.M. Warman, M.P. de Haas and J.B. Verberne (1983) Nanosecond time-resolved conductivity studies of pulse-ionized ice. 3. The electron as a probe for defects in doped ice. *Journal of Physical Chemistry,* **87**: 4096–4098.

Maeno, N. (1973) Measurement of surface and volume conductivities of single ice crystals. In *Physics and Chemistry of Ice* (E. Whalley, S.J. Jones and L.W. Gold, Ed.). Ottawa: Royal Society of Canada, p. 140–143.

Maeno, N. (1981) *The Science of Ice.* Hokkaido University Press (in Japanese).

Maidique, M.A., A. von Hippel and W.B. Westphal (1970) Transfer of protons through pure ice in single crystals, Part III. The dielectric relaxation spectra of water, ice, and aqueous solutions and their interpretation. Cambridge: Massachusetts Institute of Technology, Laboratory for Insulation Research, Technical Report 8.

Maidique, M.A., A. von Hippel and W.B. Westphal (1971) Transfer of protons through pure ice Ih single crystals. III. Extrinsic versus intrinsic polarization; surface versus volume conduction. *Journal of Chemical Physics,* **54**: 150–160.

Mogensen, O.E. and M. Eldrup (1978) Vacancies in pure ice studied by positron annihilation techniques. *Journal of Glaciology,* **21**(85): 85–99.

Muto, H., K. Matsuura and K. Nunome (1992) Large isotope effect due to quantum tunnelling in the conversion reaction of electrons to H and D atoms in irradiated H_2O/D_2O ice. *Journal of Physical Chemistry,* **96**: 5211–5213.

Nagle, J.F. (1992) Proton transport in condensed matter. In *Proton Transfer in Hydrogen–Bonded Systems* (T. Bountis, Ed.). New York/London: Plenum Press, p. 17–28.

Nilsson, G., H. Christensen, P. Pagsberg and S.O. Nielson (1972) Transient electrons in pulse-irradiated crystalline water and deuterium oxide ice. *Journal of Physical Chemistry,* **76**(7): 1000–1008.

Oguro, M., T. Hondoh and K. Azuma (Goto) (1988) Interaction between dislocations and point defects in ice crystals. *Lattice Defects in Ice Crystals* (A. Higashi, Ed.). Sapporo: Hokkaido University Press, p. 97–128.

Onsager, L. and M. Depuis (1960) The electrical properties of ice. *Termodinamica dei Processi Irreversibili.* Rendiconti della Scuola Internazionale di Fisica Enrico Fermi, Corso X, Varenna 1959. Bologna: Societa Italiana di Fisica, p. 294–315.

Petrenko, V.F. (1993a) Electrical properties of ice. USA Cold regions Research and Engineering Laboratory, Special Report 93-20.

Petrenko, V.F. (1993b) Structure of ordinary ice I_h. Part I: Ideal structure of ice. USA Cold Regions Research and Engineering Laboratory, Special Report 93-25.

Petrenko, V.F. and V.A. Chesnakov (1990) Recombination injection of charge carriers in ice. *Soviet Physics—Solid State,* **32**: 2947–2952.

Petrenko, V.F. and N. Maeno (1987) Ice field transistor. *Journal de Physique,* C1, **48**: 115–119.

Petrenko, V.F. and I.A. Ryzkhin (1984a) Dielectric properties of ice in the presence of space charge. *Physica Status Solidi (b),* **121**: 421–427.

Petrenko, V.F. and I.A. Ryzkhin (1984b) Space charge limited currents. *Soviet Physics – JETP,* **87**: 558–569.

Petrenko, V.F. and I.A. Ryzhkin (1984c) Theory of anelastic relaxation of ice. *Soviet Physics–Solid State,* **26**(9): 2681–2688.

Petrenko, V.F., R.W. Whitworth and J.W. Glen (1983) Effect of proton injection on electrical properties of ice. *Philosophical Magazine B,* **47**(3): 259–278.

Plummer, P.L.M. (1987) Quantum mechanical examination of orientational defects in ice I_h. *Journal de Physique,* C1, **48**: 46–51.

Plummer, P.L.M. (1992) Structural studies and molecular dynamics simulation of defects in ice. In *Physics and Chemistry of Ice* (N. Maeno and T. Hondoh, Ed.). Sapporo: Hokkaido University Press, p. 54–61.

Ritzhaupt, G. and J.P. Devlin (1977) Infrared spectrum of D_2O vibrationally decoupled in glassy

H_2O. *Journal of Chemical Physics*, **67**: 4779–4780.

Ritzhaupt, G., C. Thornton and J.P. Devlin (1978) Infrared spectrum of D_2O vibrationally decoupled in H_2O ice Ic. *Chemical Physics Letters*, **59**: 420–422.

Ritzhaupt, G., W.B. Collier, C. Thornton and J.P. Devlin (1980) Decoupled vibrational spectra for H_2O in D_2O ice Ic. *Chemical Physics Letters*, **70**: 294–298.

Ryzhkin, I.A. (1985) Superionic transition in ice. *Solid State Communications*, **56**(1): 57–60.

Scheiner, S. (1992) Extraction of the principles of proton transistors by ab initio methods. In *Proton Transfer in Hydrogen–Bonded Systems* (T. Bountis, Ed.). New York: Plenum Press, p. 29–47.

Scheiner, S. and J. Nagle (1983) Ab initio molecular orbital estimates of charge partitioning between Bjerrum and ionic defects in ice. *Journal of Physical Chemistry*, **87**: 4267–4272.

Schmidt, K.H. and W.L. Buck (1966) Mobility of the hydrated electron. *Science*, **51**: 70–71.

Sergienko, A.I. (1986) Soliton mechanism of Bjerrum defects motion in water molecule chains. *Ukrainskyi Fizichechui Zhurnal*, **31**: 1637–1642.

Shubin, V.N., V.A. Zhigunov, V.I. Zolotarevsky and Dolin (1966) Pulse radiolysis of crystalline ice and frozen crystalline aqueous solutions. *Nature*, **212**: 1002–1035.

Takei, I. and N. Maeno (1984) Dielectric properties of single crystals of HCL-doped ice. *Journal of Chemical Physics*, **81**: 6186–6190.

Takei, I. and N. Maeno (1987) Electric characteristics of point defects in HCl-doped ice. *Journal de Physique*, C1, **48**(3): 121–126.

Taub, I. A. and K. Eiben (1968) Transient solvated electron, hydroxyl, and hydroperoxy radicals in pulse-irradiated crystalline ice. *Journal of Chemical Physics*, **49**: 2499–2513.

Taubenberger, R., M. Hubmann and H. Gränicher (1973) Effect of hydrostatic pressure on the dielectric properties of ice I_h single crystals. In *Physics and Chemistry of Ice* (E. Whalley, S.J. Jones and L.W. Gold, Ed.). Ottawa: Royal Society of Canada, p. 194–198.

Verberne, J.B., H. Loman, J.M. Warman, M.P. de Haas, A. Hummel and L. Prinsen (1978) Excess electrons in ice. *Nature*, **272**: 343–344.

Von Hippel, A., D.B. Knoll and W.B. Westphal (1971) Transfer of protons through pure ice I_h single crystals. I. Polarization spectra of ice I_h. *Journal of Chemical Physics*, **54**: 134–144.

Von Hippel, A., A.H. Runck and W.B. Westphal (1973) Ice chemistry: Is ice I_h a proton semiconductor. In *Physics and Chemistry of Ice* (E. Whalley, S.J. Jones and L.W. Gold, Ed.). Ottawa: Royal Society of Canada, p. 236–241.

Waldridge, P.J. and J.P. Devlin (1988) Proton trapping and defect energetics in ice from FT-IR monitoring of photoinduced isotopic exchange of isolated D_2O. *Journal of Chemical Physics*, **88**(5): 3086–3091.

Warman, J.M., M.P. de Haas and J.B. Verbene (1980) Decay kinetics of excess electrons in crystalline ice. *Journal of Physical Chemistry*, **84**: 1240–1248.

Warman, J.M., M. Kunst, M.P. de Haas and J.B. Verbene (1982) Electron and proton conduction in ice. *Journal of Electrostatics*, **12**: 115–122.

Warman, J.M., M. Kunst and C.D. Jonah (1983) Subnanosecond time-resolved optical absorption studies of electron solvation in ice. *Journal of Physical Chemistry* **87**: 4292–4294.

Wörz, O. and R.H. Cole (1969) Dielectric properties of ice I_h. *Journal of Chemical Physics*, **51**: 1546–1551.

Zaretskii, A.V. (1991) Experimental determination of the H_3O^+ ions mobility in ice from 160 to 240 K. *Summaries of International Symposium on the Physics and Chemistry of Ice, September 1–6, Sapporo*, p. 204.

Zaretskii, A.V., V.F. Petrenko and V.A. Chesnakov (1988) The protonic conductivity of heavily KOH-doped ice. *Physica Status Solidi (a)*, **109**: 373–381.

SELECTED BIBLIOGRAPHY

Allen, A.O., M.P. de Haas and A. Hummel (1976) Measurements of ionic mobilities in dielectric liquids by means of concentric cylindrical electrodes. *Journal of Chemical Physics*, **64**(6): 2587–2592.

Apekis, L. and Pissis (1987) Study of the multiplicity of dielectric relaxation times in ice at low temperatures. *Journal de Physique C1*, **48**:125–133.

Auvert, G. and A. Kahane (1973) Discussion. In *Physics and Chemistry of Ice* (E. Whalley, S.J. Jones and L.W. Gold, Ed.). Ottawa: Royal Society of Canada, p. 270–271.

Aziev, E.A., A.V. Zaretskii, V.F. Petrenko and M.P. Tonkonogov (1987) Negative currents of thermally stimulated depolarization in NH_4 OH doped ice. *Institute of Solid State Physics of Academy of Science of USSR*. Chernogolovka.

Babcock, R.V. and R.L. Longini (1972) Equilibrium structure of polarized ice. *Journal of Chemical Physics*, **56**(1): 344–352.

Bilgram, J.H. and W.L. Buck (1966) Mobility of hydrated electrons. *Science*, **151**: 70–71.

Bilgram, J.H. (1974) Phase equilibria and point defects in ice. *Physik der Kondensierten Materie*, **18**: 263–273.

Bishop, P.G. and J.W. Glen (1969) Electrical polarization effects in pure and doped ice at low temperature. In *Physics of Ice* (N. Riehl, B. Bullemer and H. Engelhardt, Ed.). New York: Plenum Press, p. 492–501.

Bjerrum, N. (1951) Structure and properties of ice I. The position of the hydrogen atoms and zero–point entropy of ice. *K. danske Vidensk Selsk. Skr.*, **27**: 1–56.

Bockris, J. O'M. (1979) *Quantum Electrochemistry*. New York: Plenum Press.

Boyle, J.W., J.A. Ghormley, C.J. Hochanadel and J.F. Riley (1969) Production of hydrated electrons by flash photolysis of liquid water with light in the first continuum. *Journal of Physical Chemistry*, **73**(9): 2886–2890.

Chesnakov, V.A. (1990) Experimental study of physical process on ice–electron conductor interfaces. Ph.D. Dissertation. Chernogolovka: Institute of Solid State Physics.

Cole, K.S. and R.H. Cole (1941) Dispersion and absorption in dielectrics. *Journal of Chemical Physics*, **9**: 341–351.

Decroly, J.C., H.V. Granicher and C. Jaccard (1957) Caractere de la conductivite electrique de la glace. *Helvetica Physica Acta*, **30**: 465–467.

Dengel, O., U. Eckener, M. Plitz and N. Riehl (1964) Ferroelectric behaviour of ice. *Physics Letters*, **9**: 291–292.

Eiben, K. (1969) Irradiation–produced solvated electrons in ice. In *Physics of Ice* (N. Riehl, B. Bullemer and H. Engelhardt, Ed.). New York: Plenum Press, p. 184–194.

Engelhardt, H. (1973) Protonic conductivity of ice. In *Physics and Chemistry of Ice* (E. Whalley, S.J. Jones and L.W. Gold, Ed.). Ottawa: Royal Society of Canada, p. 226–235.

Engelhardt, H. and N. Riehl (1965) Space-charge limited proton currents in ice. *Physics Letters*, **14**: 20–21.

Engelhardt, H. and N. Riehl (1966) Zur Protonischen Leitfähigkeit von Eis–Eihkristallen bei tiefen Temperatures und hohen Feldstärken. *Physik der Kodensierten Materie*, **5**: 73–82.

Engelhardt, H., B. Bullemer and N. Riehl (1969) Protonic conduction of ice. Part II: Low temperature region. In *Physics of Ice* (N. Riehl, B. Bullemer and H. Engelhardt, Ed.). New York: Plenum Press, p. 430–442.

Evtushenko, A.A., M.B. Martirosyan and V.F. Petrenko (1988) Experimental study of electrical properties of ice grown in constant electric field.

Soviet Physics—Solid State, **30**: 2133–2138.

Gelin, H. and R. Stubbs (1965) Ice electrets. *Journal of Chemical Physics*, **12**: 967–971.

Ghormley, J.A. and C.L. Hochanadel (1971) Production of H, OH and H_2O_2 in the flash photolysis of ice. *Journal of Physical Chemistry*, **75**(1): 40–44.

Gruen, D.W.R. and Marcelja (1983) Spatially varying polarization in ice. *Journal of the Chemical Society, Faraday Transactions, 2*, **79**: 211–23.

Han, P. and D.M. Bartels (1990) H/D Isotope effects in water radiolysis. 2. Dissociation of electronically excited water. *Journal of Physical Chemistry*, **94**: 5824–5833.

Hubmann, M. (1975) Diffusion von Fremdsubstanz in Eis Beispiel NH_3. *Helvetica Physica Acta*, **48**: 449–450.

Inchachal, J.J. and A.H. Weber (1976) Electrical properties of KF–doped hexagonal ice. *Journal of Chemical Physics*, **64**(12): 4952–4956.

Isaev, A.N. and A.A. Levin (1992) MNDO/HB Study of proton transfer in the condensed phase of H_2O including medium effects in the combined 'supermolecule and pseudocontinuum' model. *Zhurnal Structurnoi Khimii*, **31**(1): 24–30.

Jaccard, C. (1966) Four–point method for measuring the volume and surface conductivities of a thin sample. *Zeitschrift Angewandte Mathematik und Physik*, **17**: 657–663.

Johari, G.P. and S.J. Jones (1975) Study of low temperature transitions in ice I_h by thermally stimulated depolarization measurements. *Journal of Chemical Physics*, **62**: 4213–4223.

Johari, G.P. and E. Whalley (1981) The dielectric properties of ice in the range 272–133 K. *Journal of Chemical Physics*, **75**: 1333–1340.

Kahane, A. (1969) Experimental and theoretical studies of the dc conductivity of ice. In *Physics of Ice* (N. Riehl, B. Bullemer and H. Engelhardt, Ed.). New York: Plenum Press, p. 443–449.

Kawabata, K. S. Okabe and S. Taniguchi (1972) Shoulder of optical absorption spectrum of the trapped electrons in gamma–irradiated crystalline ice. *Journal of Chemical Physics*, **57**(7): 2855–2856.

Lambert, M.A. and P. Mark (1970) *Current Injection in Solids*. New York/London: Academic Press.

Lee, C. and D. Vanderbilt (1993) Proton transfer in ice. Submitted for Publication to *Chemical Physics Letter*, **210**(1,2,3): 279–234

Loria, A., E. Mazzega, U. del Pennino and G. Andreotti (1978) Measurements of electrical properties of ice Ih single crystals by admittance and thermally stimulated depolarization techniques. *Journal of Glaciology*, **21**(85): 219–230.

Malmberg, C.G. and A.A. Maryott (1956) Dielec-

tric constant of water from 0° to 100°. *Journal of Research of the National Bureau of Standards*, **56**: 1–8.

Mounier, S. and P. Sixou (1969) A contribution to the study of conductivity and dipolar relaxation in doped ice crystals. In *Physics of Ice* (N. Riehl, B. Bullemer and H. Engelhardt, Ed.). New York: Plenum Press, p. 562–570.

Mulvaney, R., E.W. Wolff and K. Oates (1988) Sulphuric acid at grain boundaries in Antarctic ice. *Nature*, **331**(6153): 247–249.

Nagle, J.F. (1974) Dielectric constant of ice. *Journal Chemical Physics*, **61**: 883–888.

Nagle, J.F. (1979) Theory of the dielectric constant of ice. *Chemical Physics*, **43**: 317–328.

Nagle, J.F. and S. Tristram–Nagle (1983) Hydrogen bonded chain mechanisms for proton conduction and proton pumping. *Journal of Membrane Biology*, **74**: 1–14.

Noll, G. (1978) The influence of the rate of deformation on the electrical properties of ice monocrystals. *Journal of Glaciology*, **21**(85): 277–289.

Nye, J.F. (1985) *Physical Properties of Crystals*. Oxford: Clarendon Press.

Onsager, L. and L.K. Runnels (1969) Diffusion and relaxation phenomena in ice. *Journal of Chemical Physics*, **50**(3): 1089–1103.

Ossipyan, Y.A. and V.F. Petrenko (1988) The physics of ice. *Europhysics News*, **19**(5): 61–64.

Pauling, L. (1935) The structure and entropy of ice and of other crystals with some randomness of atomic arrangement. *Journal of the American Chemical Society*, **57**: 2680–2684.

Petrenko, V.F. and V.A. Chesnakov (1990a) On a nature of charge carriers in ice. *Soviet Physics–Solid State*, **32**: 2368–2373.

Petrenko, V.F. and V.A. Chesnakov (1990b) Investigations of physical properties of ice–electronic conductor interfaces. *Soviet Physics–Solid State*, **32**: 2655–2660.

Petrenko, V.F. and V.A. Chesnakov (1990c) Recombination injection of H_3O^+ and OH-charge carriers in electrolysis of water. *Dokl. Acad. Nauk (Soviet Physics—Doklady)*, **314**: 359–361.

Petrenko, V.F. and E.M. Schulson (1992) The effect of static electric fields on protonic conductivity of ice single crystals. In *Physics and Chemistry of Ice* (N. Maeno and T. Hondoh, Ed.). Hokkaido University Press, p. 149–155.

Pines, E. and D. Huppert (1985) Kinetics of proton transfer in ice via the pH-jump method: Evaluation of the proton diffusion rate in polycrystalline doped ice. *Chemical Physics Letters*, **116**(4): 295–301.

Polian, A. and M. Grimsditch (1984) New high-pressure phase of H_2O: Ice X. *Physics Review Letters*, **52**: 1312–1314.

Polian, A., J.M. Besson and M. Grimsditch (1984) *International Symposium on Solid State Physics under Pressure—Recent Advances with Anvil Devices*. Japan: Izu–Nagaoka, p. 18–21.

Quichenden, T.I., S.M. Trotman and D.F. Sangster (1982) Pulse radiolitic studies of the ultraviolet and visible emissions from purified H_2O ice. *Journal of Chemical Physics*, **77**(7): 3790–3802.

Ross, R.G. (1986) Solid phases of water. In *Water and Aqueous Solutions* (G.W. Neilson and J.E. Enderby, Ed.). Bristol: Adam Hilger, p. 63–74.

Ruepp, R. and M. Käss (1969) Dielectric relaxation of the bulk and surface conductivity of ice single crystals. In *Physics of Ice* (N. Riehl, B. Bullemer and H. Engelhardt, Ed.). New York: Plenum Press, p. 555–561.

Ryzhkin, I.A. (1992) New stages in understanding ice properties: a first principle approach. In *Physics and Chemistry of Ice* (N. Maeno and T. Hondoh, Ed.). Hokkaido University Press, p. 141–148.

Sergienko, A.I. (1987) Dynamics of Bjerrum faults and protonic ice conductivity. *Physica Status Solidi (b)*, **144**: 471–475.

Sokolov, B.A. (1976) *Radical Recombination Luminescence of Semiconductors*. Moscow: Nauka.

Steinemann, A. (1957) Dielektrische Eigenschaften von Eiskristallen. *Helvetica Physica Acta*, **30**: 581–610.

Tajima, Y., T. Matsuo and H. Suga (1982) Phase transition in KOH-doped hexagonal ice. *Nature*, **299**: 810–812.

Turner, G.J. and C.D. Stow (1986) DC conductivity of the ice surface. *Solid State Communications*, **58**: 403–405.

Vihj, A. K. (1973) *Electrochemistry of Metals and Semiconductors: The Application of Solid State Science to Electrochemical Phenomena*. New York: M. Dekker.

Von Hippel, A. (1971) Transfer of protons through pure ice Ih single crystals. II. Molecular models for polarization and conduction. *Journal of Chemical Physics*, **54**: 145–149.

Whalley, E. (1986) High density amorphous ice. In *Water and Aqueous Solutions* (G.W. Neilson and J.E. Enderby, Ed.). Bristol: Adam Hilger, p. 105–112.

Zaretskii, A.V., V.F. Petrenko, I.A. Ryzhkin and A.V. Trukhanov (1987a) Theoretical and experimental study of ice in the presence of a space charge. *Journal de Physique*, C1, **48**: 93–98.

Zaretskii, A.V., V.F. Petrenko, A.V. Trukhanov, E.A. Aziev and M.P. Tonkonogov (1987b) Theoretical and experimental study of pure and doped ice I_h by the method of thermally stimulated depolarization. *Journal de Physique*, C1, **48**: 87–91.

REPORT DOCUMENTATION PAGE

Form Approved
OMB No. 0704-0188

1. AGENCY USE ONLY (Leave blank)	2. REPORT DATE April 1994	3. REPORT TYPE AND DATES COVERED

4. TITLE AND SUBTITLE
Structure of Ordinary Ice I_h Part II: Defects in Ice
Volume 1: Point Defects

5. FUNDING NUMBERS
DAAL 03-91-G-0164

6. AUTHORS
Victor F. Petrenko and Robert W. Whitworth

7. PERFORMING ORGANIZATION NAME(S) AND ADDRESS(ES)

U.S. Army Cold Regions Research and Engineering Laboratory
72 Lyme Road
Hanover, N.H. 03755-1290

Thayer School of Engineering
Dartmouth College
Hanover, NH 03753

School of Physics and Space Research
The University of Birmingham
Birmingham, U.K.

8. PERFORMING ORGANIZATION REPORT NUMBER
Special Report 94-4

9. SPONSORING/MONITORING AGENCY NAME(S) AND ADDRESS(ES)

U.S. Army Research Office
Research Triangle Park
Durham, NC 27709

10. SPONSORING/MONITORING AGENCY REPORT NUMBER
ARO 28599.3-GS

11. SUPPLEMENTARY NOTES

12a. DISTRIBUTION/AVAILABILITY STATEMENT
Approved for public release; distribution is unlimited.
Available from NTIS, Springfield, Virginia 22161

12b. DISTRIBUTION CODE

13. ABSTRACT (Maximum 200 words)

This report examines point defects in ice: molecular defects (vacancies and interstitials), protonic point defects (ions and Bjerrum defects) and electronic point defects (solvated electrons and radicals). Experimental results and theoretical models of the defects' atomic and electronic structures, energies and mobilities are reviewed. Special attention is given to the results of studies from the last two decades. Among the experimental techniques under consideration are nuclear magnetic resonance, X-rays topography, electron spin resonance, measurements of ice conductivity and dielectric permittivity, spectra of optical absorption and photoluminescence and measurements of diffusion coefficients of the oxygen and hydrogen isotopes in ice. Ab initio calculations, computer simulations, Jaccard's theory and soliton models are used to discuss the defects' structures and their properties.

14. SUBJECT TERMS
Ice
Ice physics
Molecular structure
Point defects

15. NUMBER OF PAGES
45

16. PRICE CODE

17. SECURITY CLASSIFICATION OF REPORT	18. SECURITY CLASSIFICATION OF THIS PAGE	19. SECURITY CLASSIFICATION OF ABSTRACT	20. LIMITATION OF ABSTRACT
UNCLASSIFIED	UNCLASSIFIED	UNCLASSIFIED	UL